Data on 17 Icelandic volcanic glasses and 1 Californian ignimbrite

RH-03-2004

Domenik Wolff-Boenisch

Science Institute, University of Iceland, Dunhaga 3,
107 Reykjavik

European Research Training Network "Quantifying the dissolution and precipitation of solid solutions in natural and industrial processes"
(5FP, contract number: HPRN-CT-2000-00058)

Data on 17 Icelandic volcanic glasses and 1 Californian ignimbrite

RH-03-2004

Domenik Wolff-Boenisch

Science Institute, University of Iceland, Dunhaga 3,
107 Reykjavik

May 2004

Table of Contents

Index of Tables

Introduction

This internal report contains a compilation of volcanic glass related data that was generated during the author's research stay at the Science Institute, University of Iceland, from 2001-2004. Most of this data has not found its way in a published manuscript but the author feels that it should be available as a reference source as it contains valuable information on volcanic glasses that are all but one from Iceland. In this respect the author expresses his gratitude to the following Icelanders: Sigurdur Gislason from the Science Institute for offering the author the opportunity to carry out this project and for this continuous support throughout these three years. Gudrun Larsen from the Science Institute whose contribution was vital to finding adequate sample outcrops. With her invaluable knowledge, pumices and ash layers of six Hekla, two Katla, one Öraefajökull, and one Eldgjá eruptions were sampled. Moreover did she kindly provide the author with ash samples from the Grimsvötn 1998 and Hekla 2000 eruptions. Thanks goes also to Sveinn Jacobsson from the Natural History Museum of Iceland for sharing his precious ashes from the Heimaey 1973 and Surtsey 1964 eruptions. Olgeir Sigmarsson from the Science Institute endowed the author with the only foreign glass from an ignimbrite flow in the Long Valley, California. In total 18 volcanic glasses were available for a study on dissolution kinetics and results thereof can be found in Wolff-Boenisch et al. (2004a, 2004b). This internal report is meant as a supplement to the data published in these papers.

Sample Location

Table 1 Geographical coordinates and description of the sample locations

	N	W	
Bishop Tuff	-	-	Pumice chunks (decimeters in diameter) sampled from the fall deposits exposed in the Chalfant Valley, Long Valley Caldera, California (1g1Eb). For reference see Wilson and Hildreth (1997), J. Geol. 105, 403-439.
Öraefajökull 1362	63.54.11	16.36.03	W of the farm Hnappavelllir. It is a small quarry, sample consists of large chunks and represents the airborne phase of the eruption (50-60 cm above the soil at the bottom of quarry).
Hekla 1104	64.03.28	19.46.29	In a slope down to Ytri-Rangá, close to a track leading down to a bridge. Sample from the lowermost 20 cm of the layer.
Hekla 3W and 3B	64.04.15	19.45.46	Pumice quarry (3.5 m thick). Brown pumice picked 70 cm from the top; white pumice sampled at the bottom of the quarry.
Askja 1875	65.02.37	16.43.09	Pumice (decimeters in diameter) sampled from the S rim of the explosion crater Viti. The 4 m section is in the upper part of a steep slope. GPS point about 300 m southeast of the sample spot.
Silk-LN	63.49.7	18.37.4	In a 10 m deep gully cut in sediment in terraces W of River Thorvaldsá on Landmannaleid, Skaftártunguafrétti. The ash layer was 10 cm thick.
Hekla 2000	64.08.87	19.33.12	Ash sampled just within the 3 cm isopach, collected on snow to prevent any interaction with soil/meltwater.
Hekla Z0, Z1, Z3	64.02.20	19.20.20	SW of the intersection of the mountain tracks Dómadalur and Krakatindur. Sampled from 3 m high section on the west bank of a small stream. X is at the top, then y and z represents the lower half of the section.
Grimsvötn 1998	-	-	At the W rim of the 1998 crater, sampled at the surface and in shallow depth.
Heimaey 1973	-	-	Scoria taken from the very initial phase of the Eldfell eruption (23.01.73) on the stairs of the farm Kirkjubaer on Heimaey, Vestmanneyar Islands.
Askja 1961	65.04.06	16.43.27	Scoria samples from the E rim of the spatter cone just SE of the parking lot in Vikraborgir. GPS point about 200 m north-west of sampling spot.
Krafla 1984	65.43.5	16.48.4	Scoria, sampled from a small crater W of the eruption crater Hófur and north of Leirhnukur.
Katla 1755	63.37.9	18.30.7	In Hrífuneshólmi in Skaftártunga. Sample taken on the E side of a small gully running S from Hómsá. The track runs down to the river in the gulley. Sample taken at 65 cm depth from the surface.
Surtsey 1964	-	-	Bomb fallen between 14.-28.02.1964. Found on the W rim of the crater Surtur II on the Island Surtsey, Vestmanneyar Islands.
Eldgjá 934	63.56.99	18.39.33	In a steep gully S of the main Landmannaleid track as it "climbs" up the west bank of the Eldgjá fissure. GPS point is at the top of the hill.

Chemical Composition

Table 2 XRF chemical analyses of the major elements of the volcanic glasses in weight percent

Sample*	Code	SiO_2	TiO_2	Al_2O_3	Fe_2O_3	FeO	MnO	MgO	CaO	Na_2O	K_2O	P_2O_5	LOI
Bishop Tuff, 0.76 Ma#	BT	72.62	0.08	12.48	0.78	0.11	0.03	0.09	0.48	3.79	4.38	0.01	4.83
Öraefajökull 1362	Ö62	70.64	0.24	13.00	2.40	1.18	0.10	0.02	0.97	5.45	3.41	0.02	1.95
Hekla 1104	H1	70.59	0.22	13.78	1.10	2.28	0.11	0.09	1.92	4.88	2.67	0.04	1.40
Hekla 3W, 2900 BP	H3W	69.79	0.21	13.79	1.15	2.32	0.11	0.11	2.08	4.83	2.48	0.04	1.90
Askja 1875	A75	69.28	0.90	12.42	2.48	2.09	0.10	0.97	2.81	3.74	2.21	0.19	1.70
Hekla 3B, 2900 BP	H3B	66.01	0.42	14.65	2.14	3.81	0.18	0.39	3.21	4.72	2.07	0.10	0.97
Hekla Z0, 2300 BP	HZ0	62.80	0.96	15.34	2.64	4.53	0.17	1.40	4.57	4.35	1.55	0.34	0.20
Silk-LN, 3100 BP	SLN	62.76	1.26	14.36	2.09	4.15	0.19	1.05	2.94	4.62	2.55	0.30	2.64
Hekla 2000†	H20	54.81	1.98	14.35	4.38	7.48	0.27	2.81	6.65	4.01	1.27	0.96	-0.43
Hekla Z1, 2300 BP	HZ1	54.14	2.00	14.81	6.31	5.55	0.26	2.93	6.53	3.66	1.20	1.01	0.20
Hekla Z3, 2300 BP	HZ3	51.62	2.36	14.49	6.00	7.11	0.28	3.30	6.96	3.29	1.06	1.27	0.57
Grimsvötn 1998†	GR	50.77	2.53	13.55	2.57	10.26	0.20	5.54	9.87	2.77	0.52	0.28	-0.93
Heimaey 1973†	HEI	50.48	2.24	16.16	3.78	7.77	0.25	2.54	6.94	5.84	1.60	0.78	-0.23
Askja 1961	A61	50.13	2.73	12.74	4.91	10.73	0.24	4.66	8.97	2.70	0.56	0.31	-0.70
Krafla 1984	KRA	49.78	2.01	13.44	3.06	11.56	0.23	5.73	10.23	2.37	0.32	0.20	-0.87
Katla 1755	KAT	47.07	4.50	12.65	4.13	11.08	0.23	4.79	9.11	2.79	0.77	0.64	0.00
Surtsey 1964†	SS	46.48	2.46	16.35	2.57	9.66	0.19	5.88	9.87	3.60	0.67	0.33	-0.13
Eldgjá 934	ELD	46.09	4.35	12.98	6.11	9.65	0.21	5.31	10.15	2.59	0.66	0.44	-0.26

#van den Bogaard and Schirnick (1995)

*Sample names consist of the sample location and eruption date. 0.76 Ma refers to 0.76 million years before present, 2900 BP stands for 2900 years before present, and 1104 represents the year 1104. Exact dates of eruptions occurring before 934 are somewhat uncertain.

†Specimens from these eruptions were taken days to weeks after the volcanic activity, i.e. eruption age does not equal weathering age

Table 3 XRF chemical analyses of the trace elements of the volcanic glasses in parts per million

Sample	Code	Sc	V	Cr	Co	Ni	Cu	Zn	Ga	Rb	Sr	Y	Zr	Nb	Ba	La	Ce	Pr	Nd	Sm
Bishop Tuff, 0.76 Ma	BT	3	7	1	1	1	6	29	15	146	20	23	84	20	32	29	48	3	21	6
Öraefajökull 1362	Ö62	1	3	4	1	3	6	166	28	76	58	110	746	76	657	80	157	15	82	19
Hekla 1104	H1	5	2	0	0	4	21	127	24	57	163	86	488	74	628	81	165	15	80	14
Hekla 3W, 2900 BP	H3W	8	2	3	2	5	18	124	23	53	170	83	464	70	605	78	157	15	77	13
Askja 1875	A75	14	44	5	7	6	17	80	16	52	108	58	363	31	334	40	84	5	37	10
Hekla 3B, 2900 BP	H3B	13	4	0	8	2	12	158	25	44	243	79	758	68	529	68	143	13	68	15
Hekla Z0, 2300 BP	HZ0	15	31	3	9	5	22	127	23	33	292	59	449	47	369	50	109	8	53	12
Silk-LN, 3100 BP	SLN	7	30	1	5	3	1	167	26	55	294	77	800	101	523	78	170	15	84	18
Hekla 2000	H20	24	66	0	15	5	5	187	25	24	368	74	467	63	300	51	126	10	67	15
Hekla Z1, 2300 BP	HZ1	22	84	0	18	1	5	178	24	22	359	70	442	56	284	49	123	12	64	14
Hekla Z3, 2300 BP	HZ3	25	96	0	21	6	8	196	25	21	370	77	440	62	248	49	130	14	67	18
Grimsvötn 1998	GR	39	371	53	44	38	94	129	21	9	225	42	209	21	62	15	55	4	20	7
Heimaey 1973	HEI	21	49	1	15	4	11	168	27	35	315	69	444	52	305	41	111	10	55	13
Askja 1961	A61	45	468	27	48	35	129	180	21	11	185	45	188	23	77	15	53	5	21	12
Krafla 1984	KRA	42	407	116	53	54	121	129	20	5	158	38	116	14	44	8	38	0	10	6
Katla 1755	KAT	30	392	0	44	26	34	164	25	16	429	44	271	40	108	28	88	11	41	8
Surtsey 1964	SS	32	283	144	39	64	40	109	21	13	345	35	187	23	110	15	58	3	24	7
Eldgjá 934	ELD	27	402	11	50	45	111	152	22	12	392	38	224	32	60	20	62	3	29	6

Surface Areas

Table 4 Summary of physical properties of the glass powders (45-125 μm) used in this study

sample	volcanic name	glass density* g/cm^3	A_{BET} cm^2/g/10^4	A_{geo} cm^2/g	roughness factor	pH_{zpc}
BT	rhyolite	2.31	3.12	332	94	6.9
Ö62	rhyolite	2.36	0.43	324	13	7.4
H1	rhyolite	2.42	0.56	317	18	7.0
H3W	rhyolite	2.42	1.08	316	34	6.9
A75	rhyolite	2.45	1.41	312	45	7.0
H3B	dacite	2.51	1.21	305	40	6.9
HZ0	dacite	2.59	0.62	296	21	7.0
SLN	dacite	2.55	2.65	301	88	6.9
H20	b-andesite	2.79	0.12	275	4	7.0
HZ1	b-andesite	2.73	2.16	280	77	6.9
HZ3	basalt	2.81	4.34	273	159	7.0
GR	basalt	2.99	0.11	256	4	7.0
HEI	mugearite	2.81	0.07	272	3	6.9
A61	basalt	2.99	0.14	256	6	6.9
KRA	basalt	3.04	0.14	252	6	7.0
KAT	basalt	3.04	0.94	252	37	6.9
SS	basalt	3.00	0.19	255	8	6.9
ELD	basalt	3.02	5.22	253	206	7.0

*corresponds to the particle density, not corrected for potential vesicularity

"b-" means "basaltic", pH_{zpc} is the zero point of charge, roughness factor is the ratio of A_{BET}/A_{geo}

SEM

The samples have all been ground, dry sieved to the 45-125 μm size fraction and ultrasonically cleaned in acetone and deionised water. Specimens were examined at different magnifications in a JEOL JSM 6300F at 20kV.

Roughly there exist three groups of glasses:

1) Glasses revealing a smooth, uncoated, and bubble-free surface, which is consistent with their low roughness factors (H20, GR, HEI, A61, KRA, SS).
2) Glasses which are also smooth and uncoated but which exhibit porosity due to the presence of bubbles. Consequently, the surface roughness of these glasses is bigger (Ö62, H1, H3W, A75, H3B, HZ0, KAT).
3) Glasses with significant weathering features (BT, SLN, HZ1, HZ3, ELD). As a result, the roughness factors are very high. EDX analyses show the surface coatings to be iron non-silicates.

For the glasses of the third group four images are provided to illustrate the weathering features while only two photos, an oversight and a characteristic grain, represent the glasses from the two other groups. The order of the images follows the silica content (cf. Table 2), i.e. starting with the rhyolitic glasses, and the code of each glass is shown on the image. For the basaltic glasses HZ3 and ELD backscattering images are also added at the end. They reveal plagioclase lathes and opaque Ti/Fe-ores within the glassy matrix. Table 5 is a rough subjective characterization of the porosity, smoothness, and coating of each glass and sets the base for the classification into the three groups presented above.

Table 5 Visual assessment of the porosity, smoothness, and coating of the volcanic glasses

Sample	porous	smooth	coated
BT	+	-	-
Ö62	±	+	-
H1	++	+	-
H3W	++	+	-
A75	+	+	-
H3B	++	+	-
HZ0	+	+	-
SLN	+	±	±
H20	-	±	-
HZ1	±	-	+
HZ3	-	-	±
GR	-	+	-
HEI	-	+	-
A61	-	±	-
KRA	-	+	-
KAT	+	+	-

SS	-	+	-
ELD	-	-	+

++ = very, + = markedly, ± = not markedly, - = not

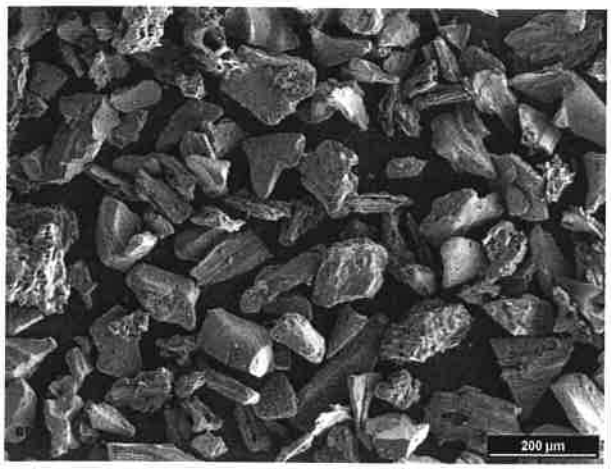
200 µm

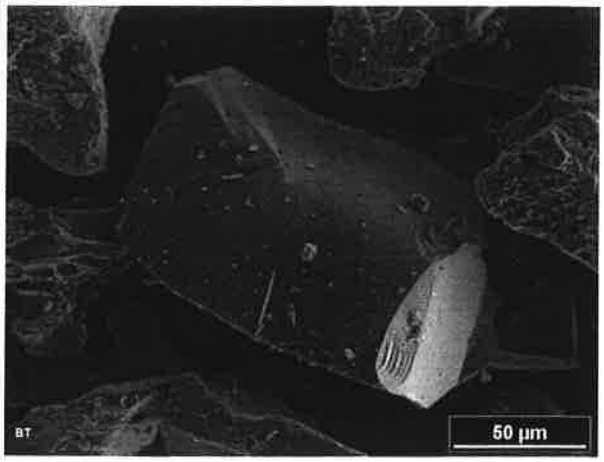
50 µm

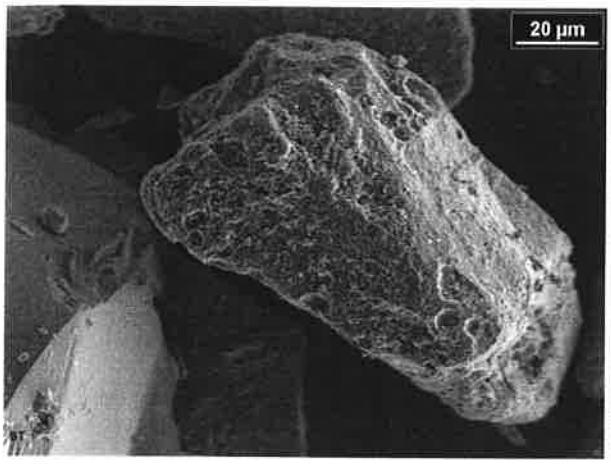
20 µm

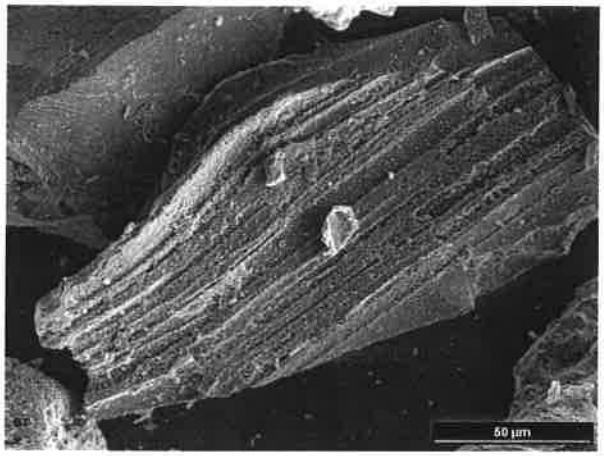
50 µm

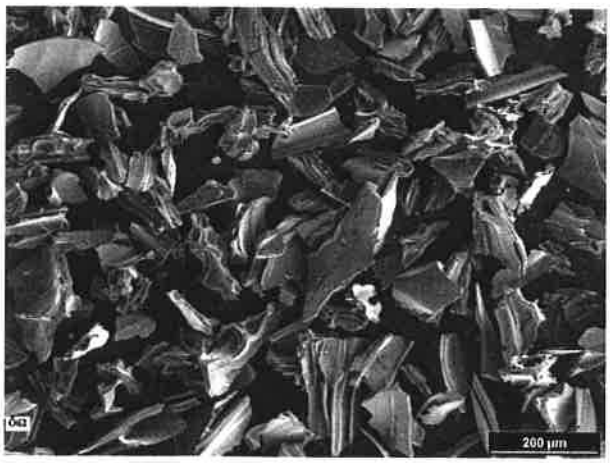
200 µm

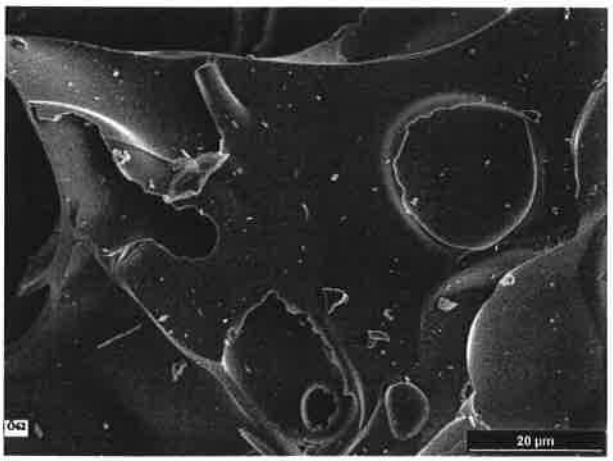
20 µm


200 µm

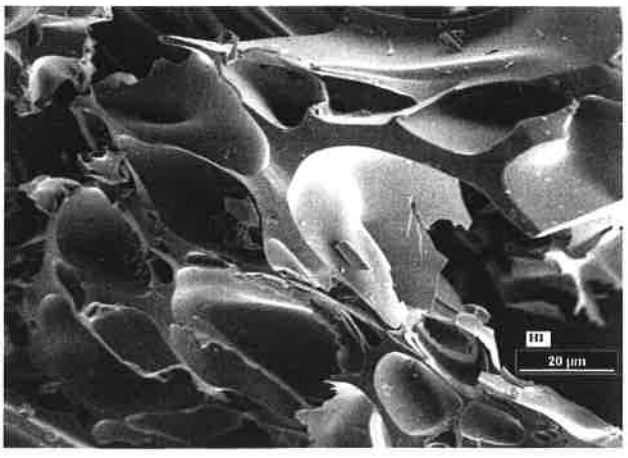
20 µm


H3W
200 µm

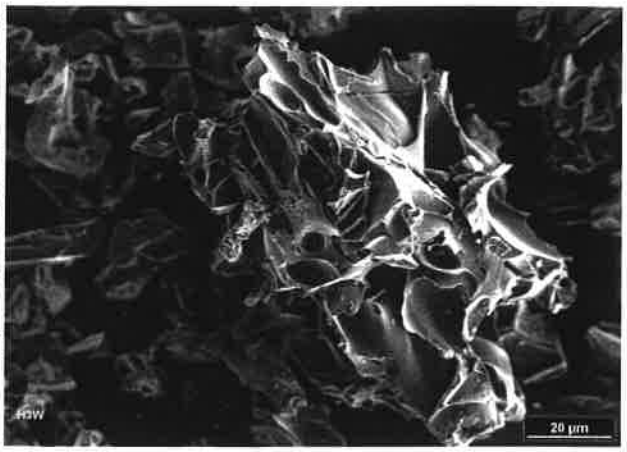
H3W
20 µm

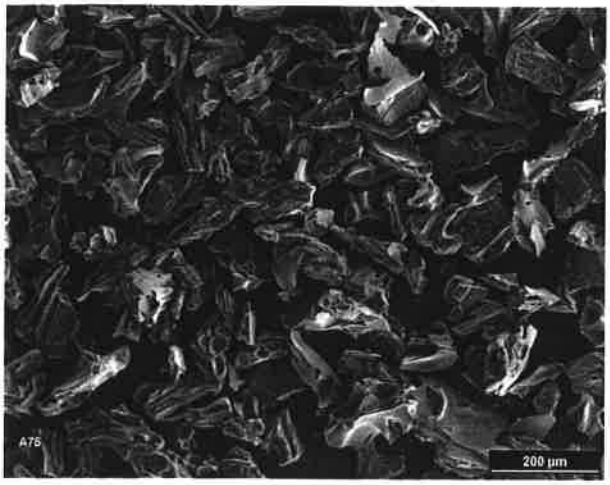
A75
200 µm

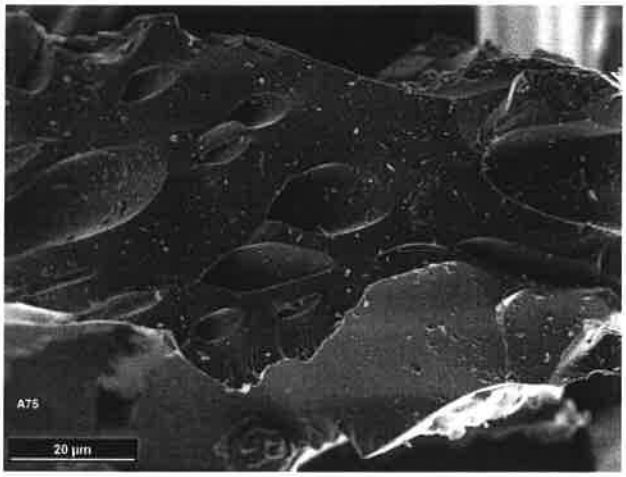
A75
20 µm

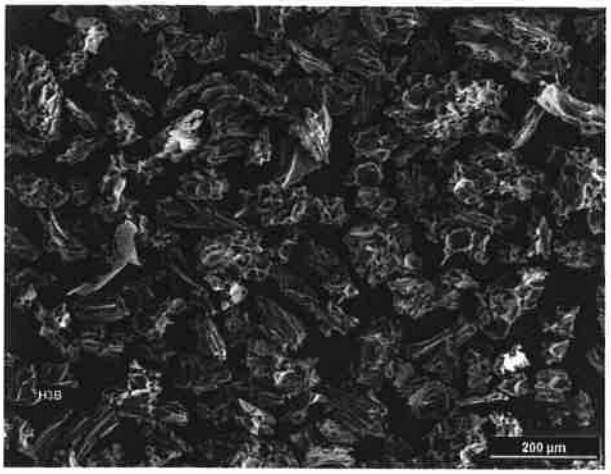
H3B
200 µm

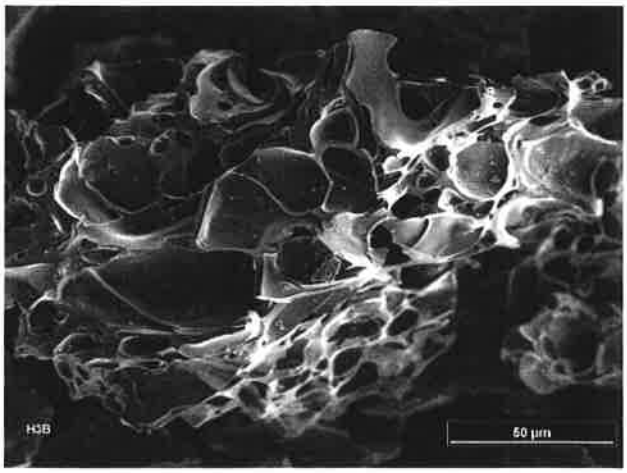
H3B
50 µm


200 µm
HZ0

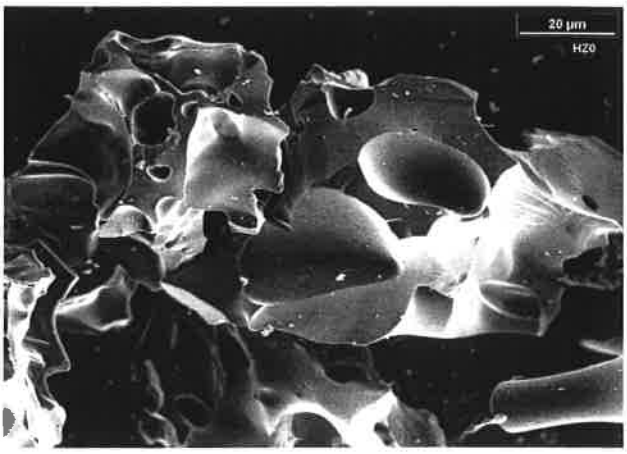
20 µm
HZ0


SLN
200 µm

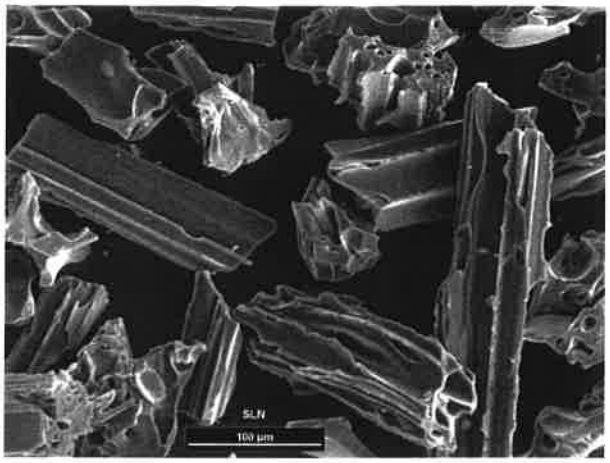
SLN
100 µm

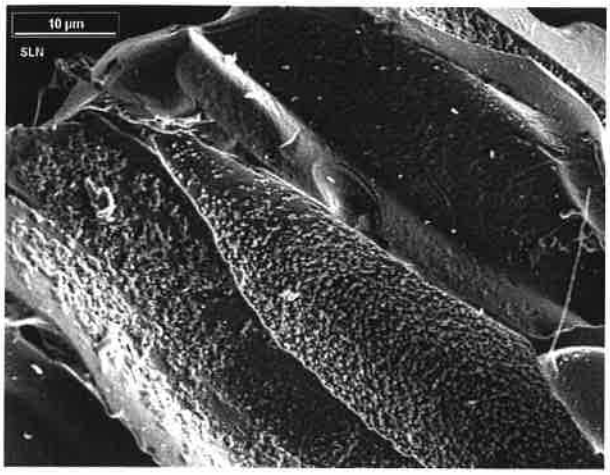
10 µm
SLN

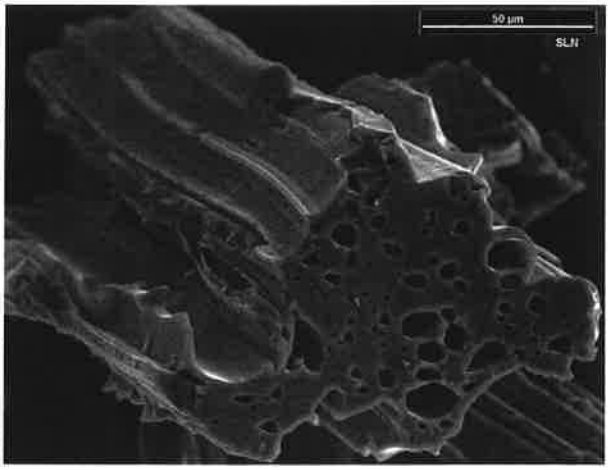
50 µm
SLN

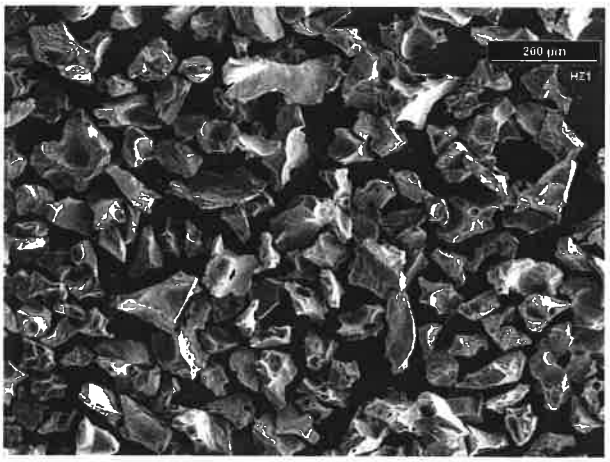
200 µm
HZ1

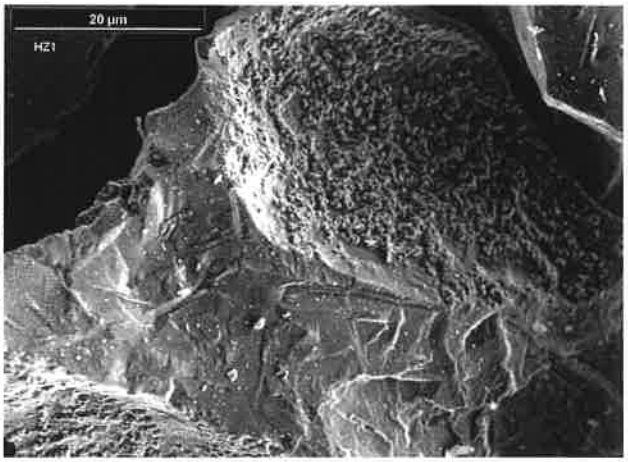
20 µm
HZ1

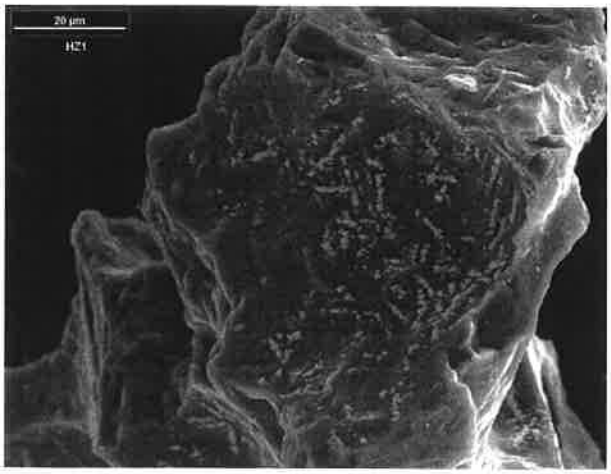
20 µm
HZ1

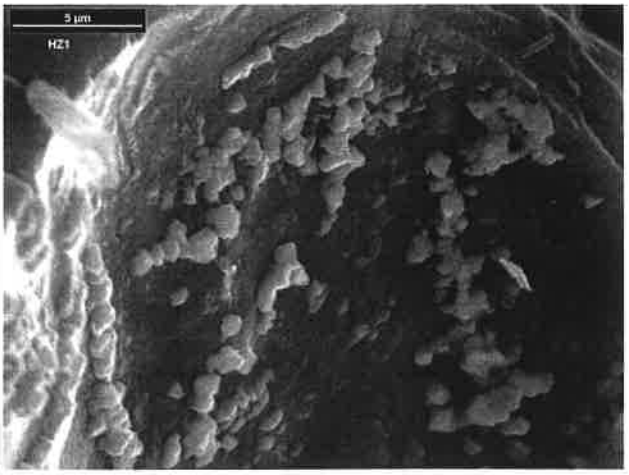
5 µm
HZ1

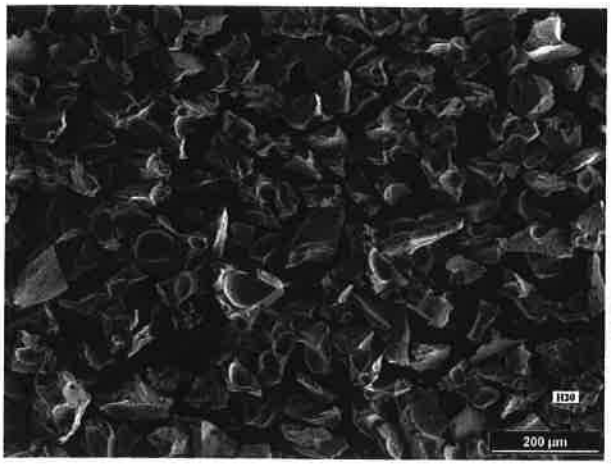
H20
200 µm

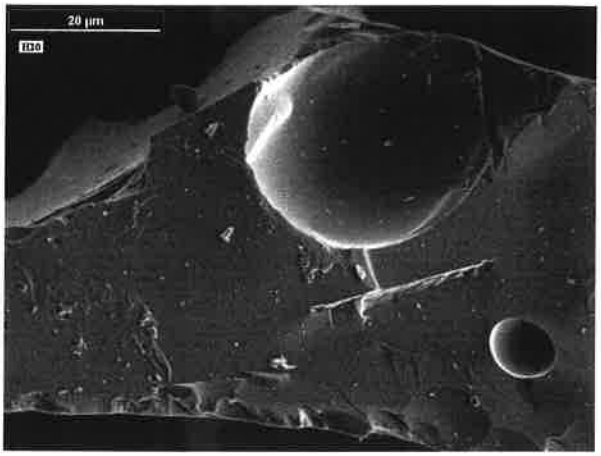
20 µm
H20

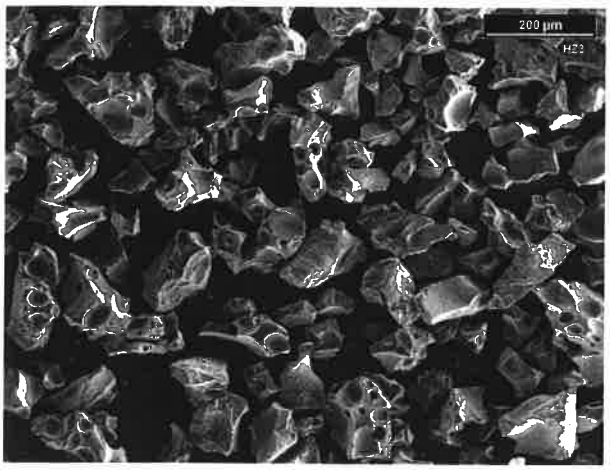
200 µm
HZ3

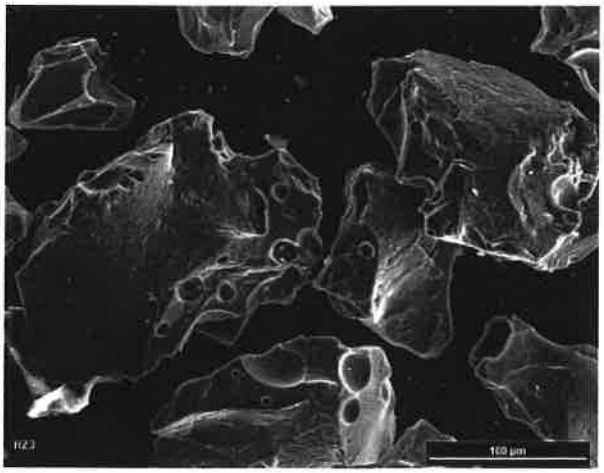
HZ3
100 µm

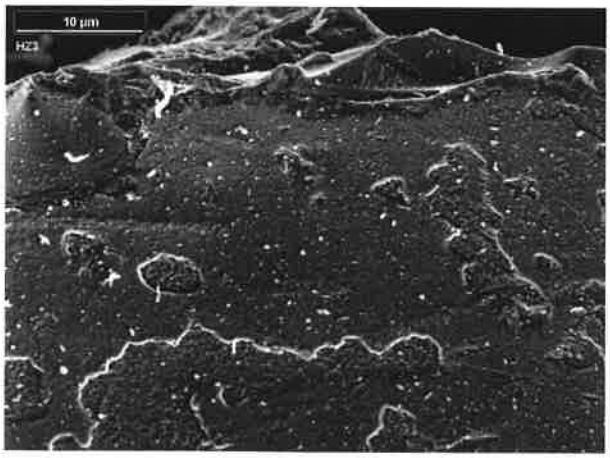
10 µm
HZ3

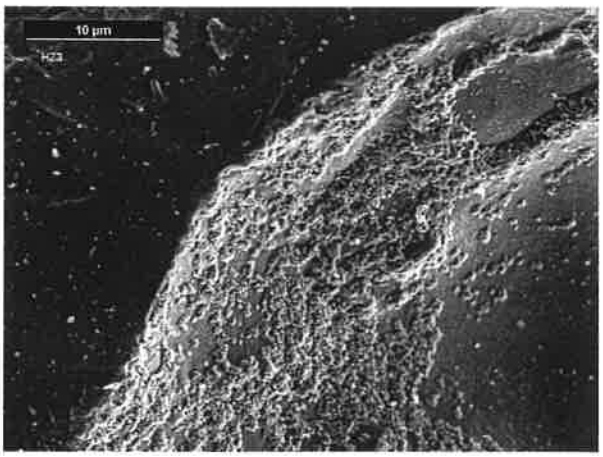
10 µm
HZ3

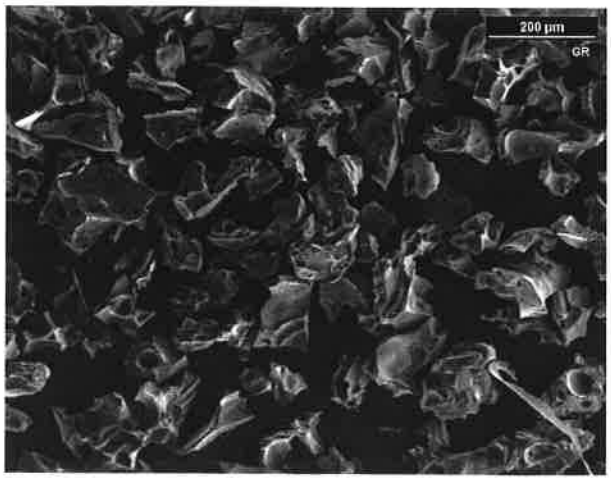
200 µm
GR

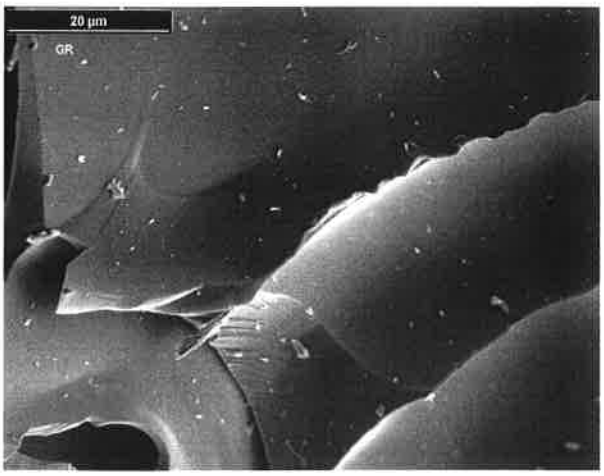
20 µm
GR

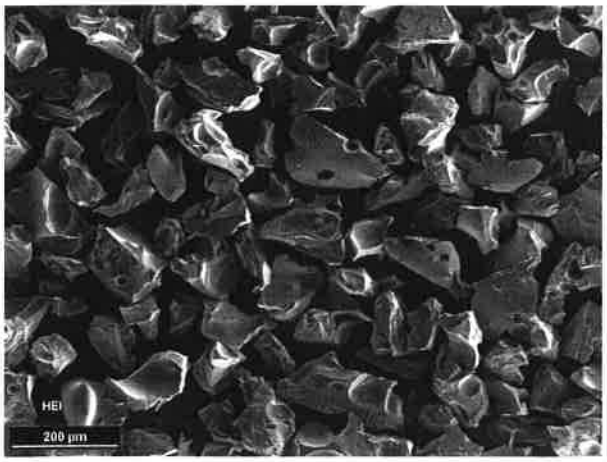
HEI
200 µm

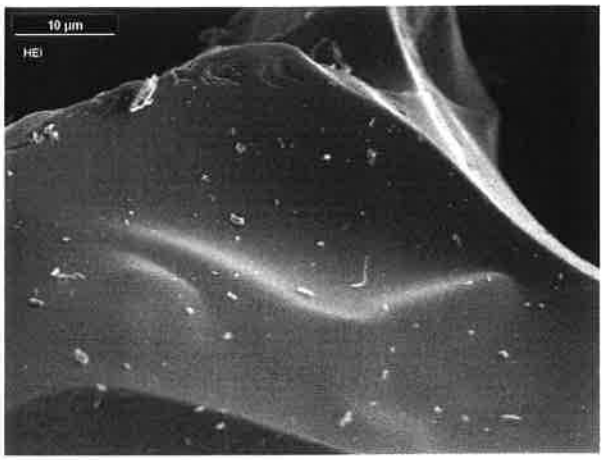
10 µm
HEI

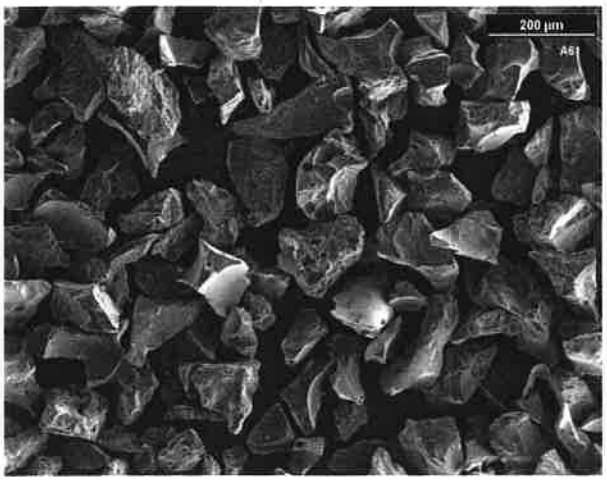
200 µm
A61

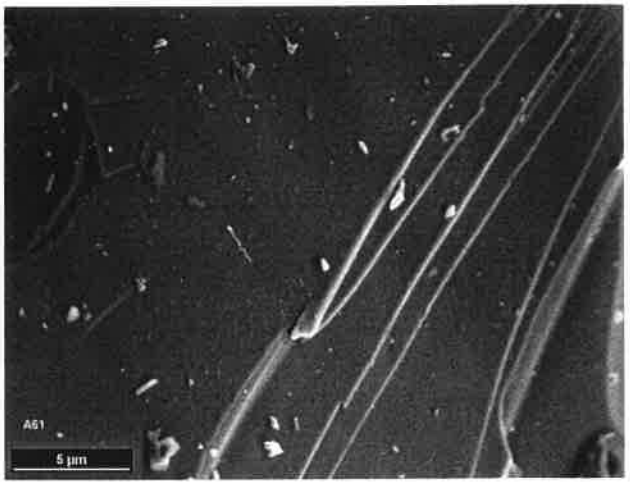
A61
5 µm

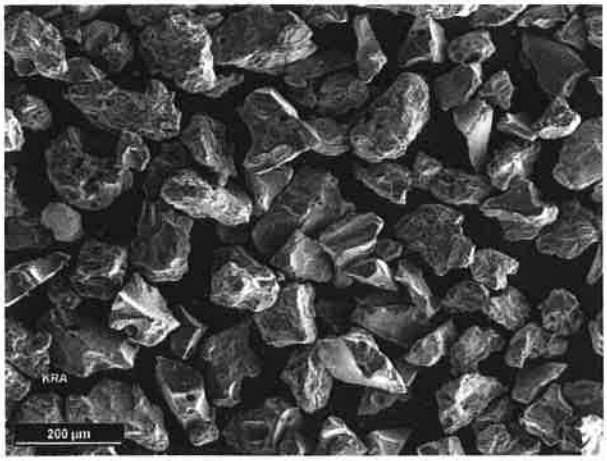
KRA
200 µm

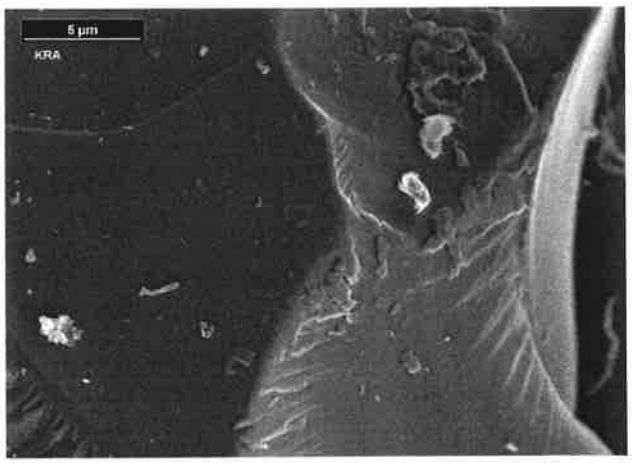
5 µm
KRA

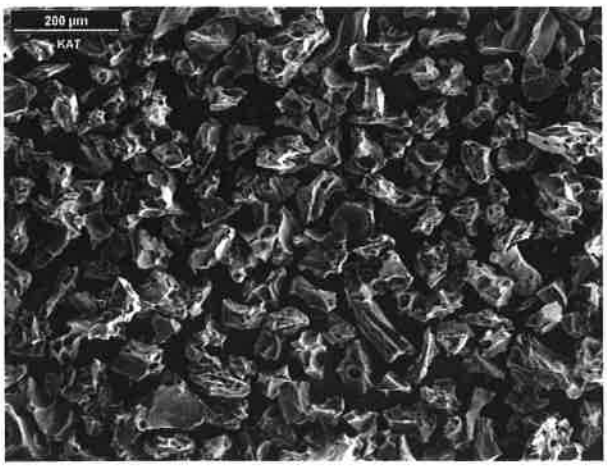
200 µm
KAT

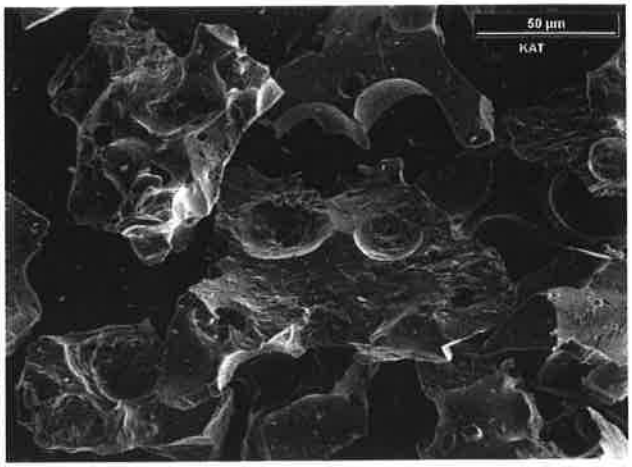
50 µm
KAT

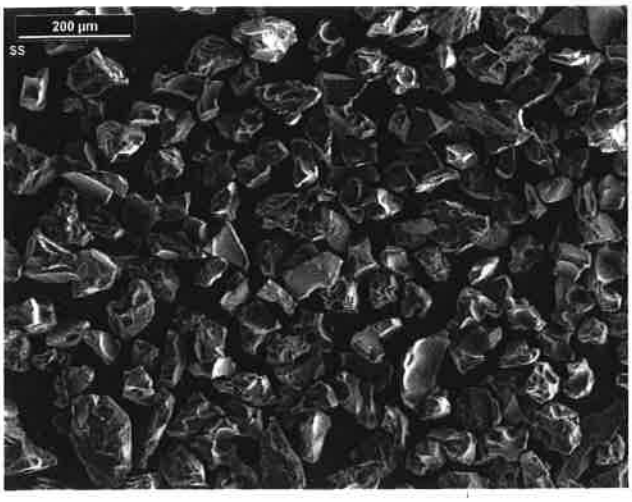
200 µm
SS

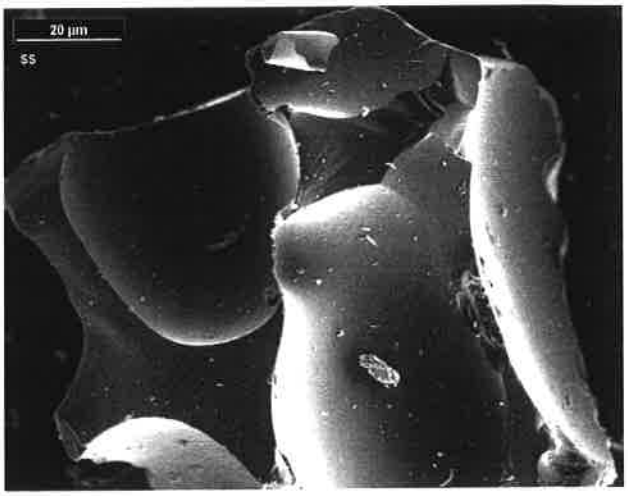
20 µm
SS

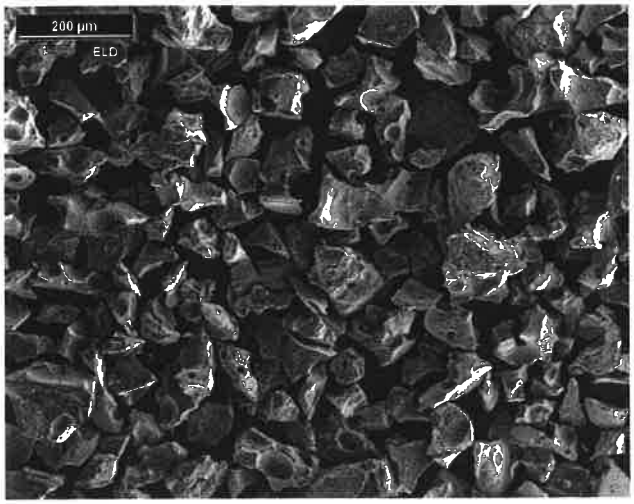
200 µm
ELD

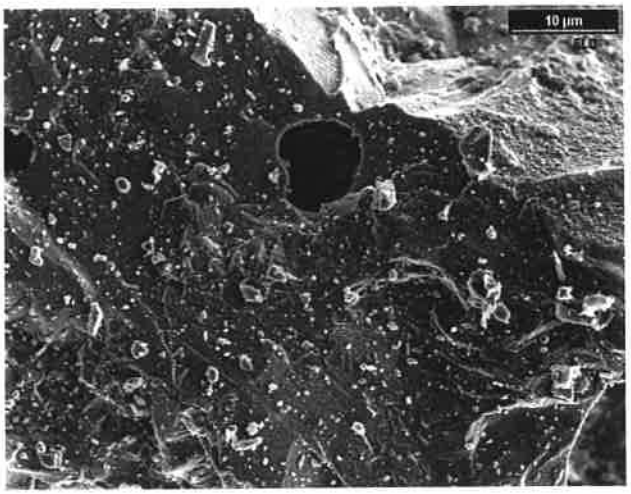
10 µm
ELD

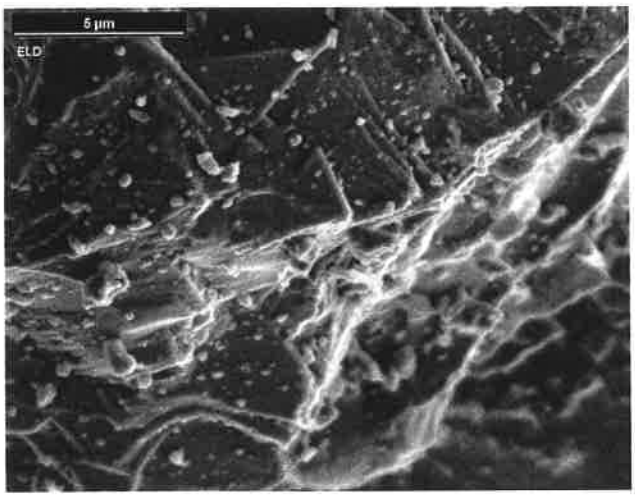
5 µm
ELD

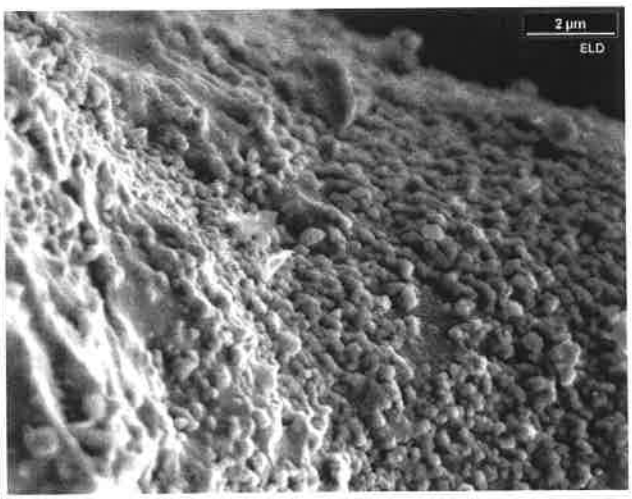
2 µm
ELD

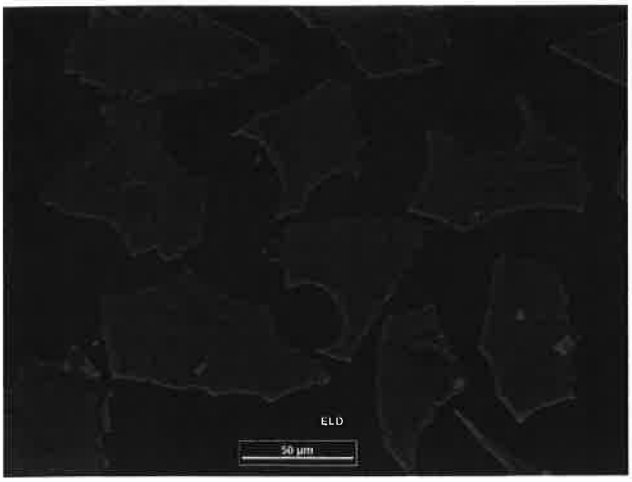
ELD
50 µm

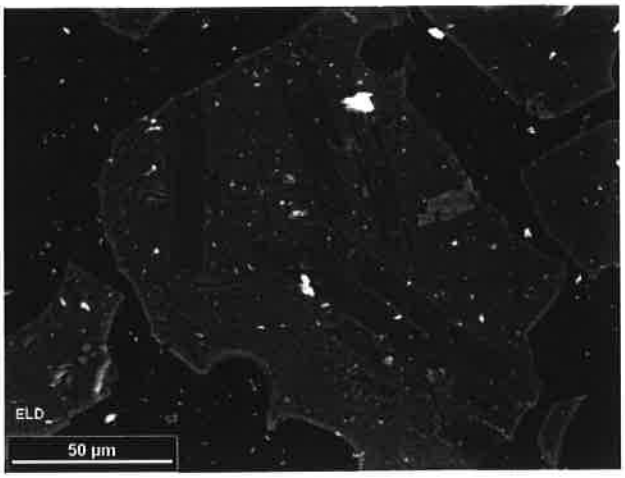
ELD
50 µm

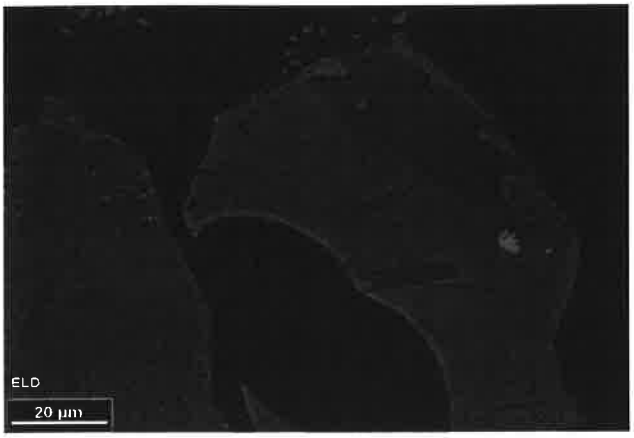
ELD
20 µm

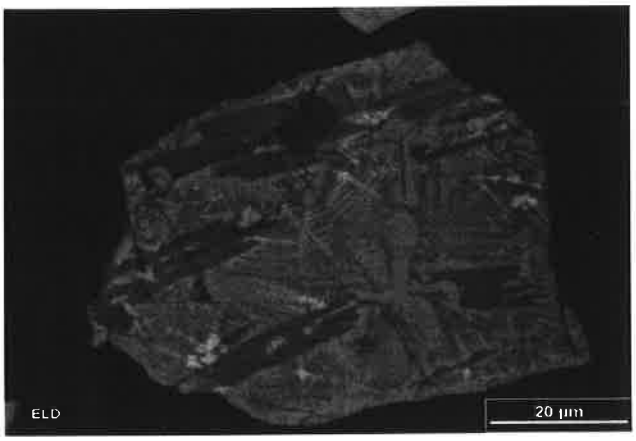
ELD
20 µm

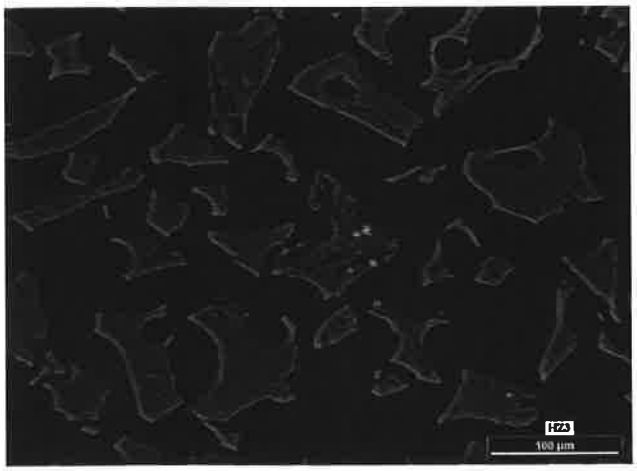
HZA
100 µm

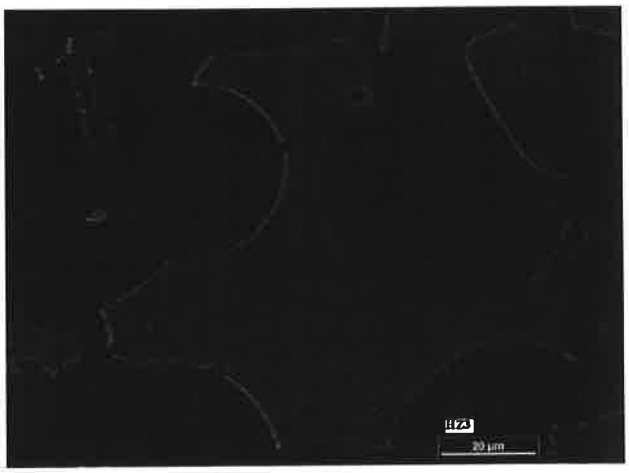
HZA
20 µm

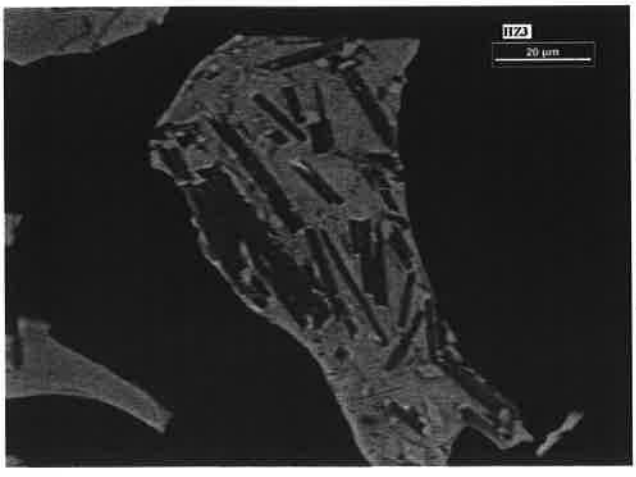
HZA
20 µm

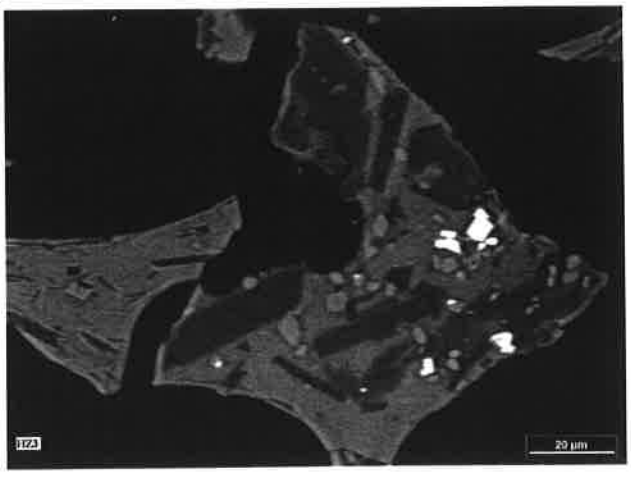
HZA
20 µm

Surface Titration

Surface titrations on the 18 volcanic glasses were carried out to determine their zero point of charge (pH_{zpc}). This is the pH at which the glass surface has no net electrical charge because the sum of negatively and positively charged surfaces cancels out. Experiments were performed in 250 ml acid washed plastic beakers filled with 100 ml of a 1mM NaCl background electrolyte solution to which 1 gram of glass (45-125 μm size fraction) was added. The suspension was magnetically stirred and continuously purged with N_2 during the experiment to prevent CO_2 entering. Once the pH meter marked a constant value and the suspension had stabilized (usually after 20-30 min) the titration was started by adding stepwise $HClO_4$ with a micropipette in different concentrations (1, 10, 100 mM) until the pH dropped to a low value (black diamonds in the figures). Back titrations were performed then by adding NaOH in the same way until reaching a high pH (open circles in the figures). From there $HClO_4$ was added again until the pH reached its initial value (black diamonds in the figures).

The most important aspect of titration experiments is the effect of atmospheric CO_2 and the related essential stabilization of the pH. The initial phase of the titration experiments is therefore very crucial as both the N_2 bubbling rate as well as the stirring rate determines the exposed surface of the suspension and thus the amount of CO_2 that can be in contact with the surface. The greatest error occurs if the starting pH of the *equilibrated* suspension is not determined correctly. Furthermore does the addition of only small concentrations of acid in the beginning only cause minor changes in the pH and if these are not assessed accurately the whole titration becomes questionable. Another aspect is the rapid initial dissolution of high surface energy sites on the glass surface, which consumes protons. The pH_{zpc} of the glasses lies apparently between 6-8 (see figures that follow) and the precise values provided in table 2 agree well with the work of Guy and Schott (1989) who give a pH_{zpc} of 6.8 for basaltic glass. Still, caution must be exercised as these pH_{zpc} values lie suspiciously close to the neutral pH and do not change from basalts to rhyolites; therefore they might wear artefacts stemming from the influence of bubbling and stirring.

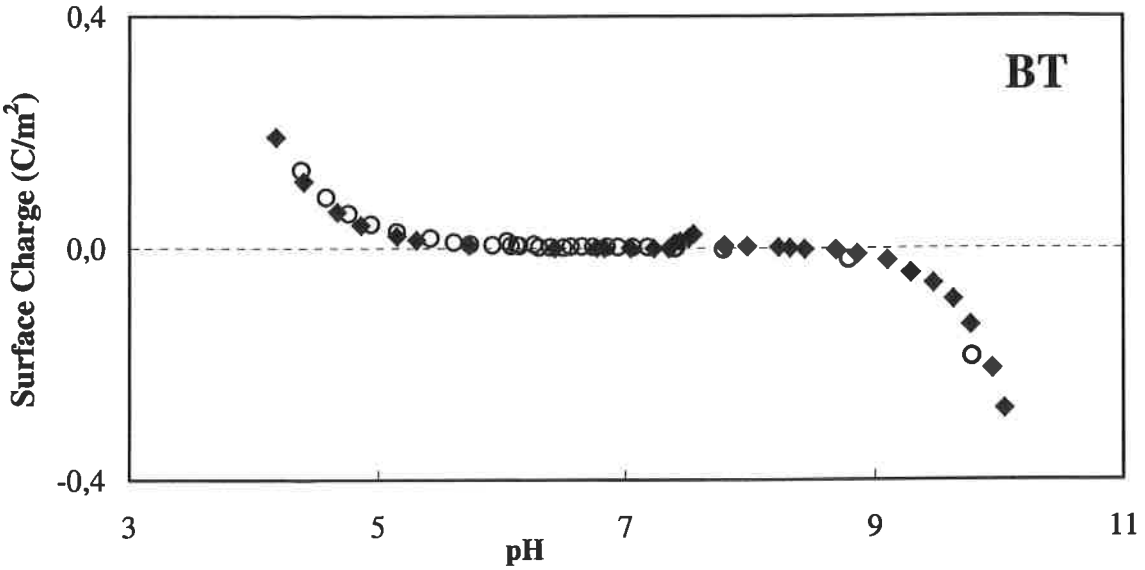
BT
0,4
0,0
-0,4
Surface Charge (C/m²)
3
5
7
9
11
pH

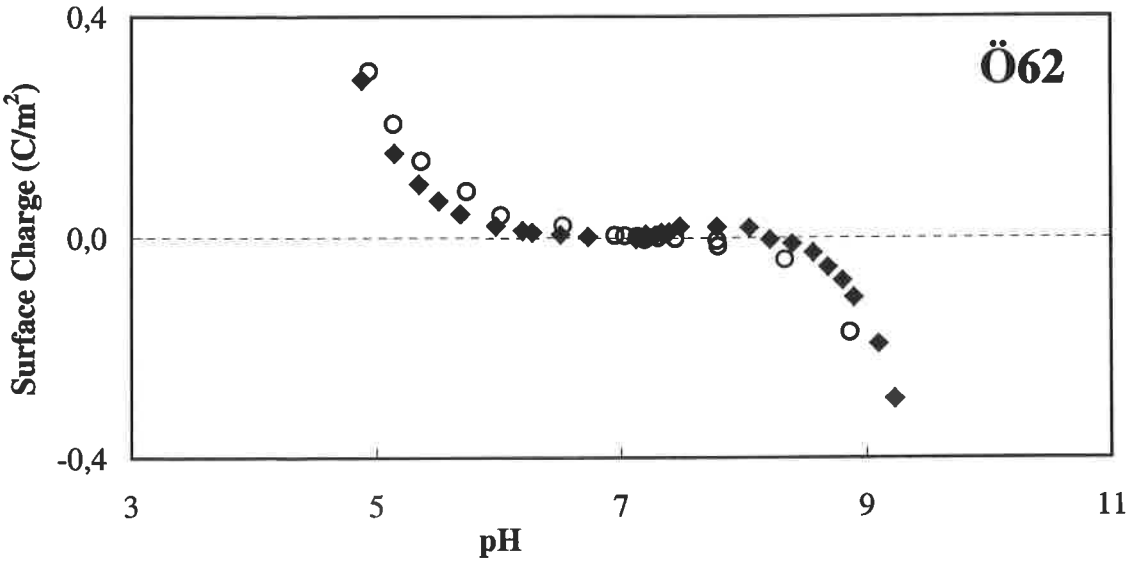
Ö62
0,4
0,0
-0,4
Surface Charge (C/m²)
3
5
7
9
11
pH

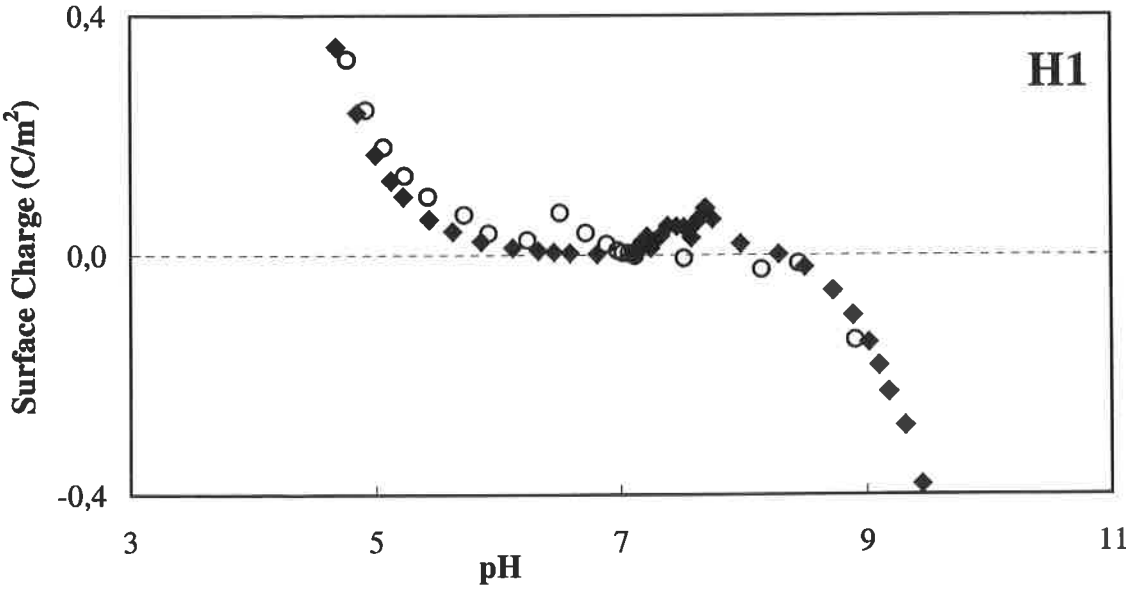
H1
0,4
0,0
-0,4
Surface Charge (C/m²)
3
5
7
9
11
pH

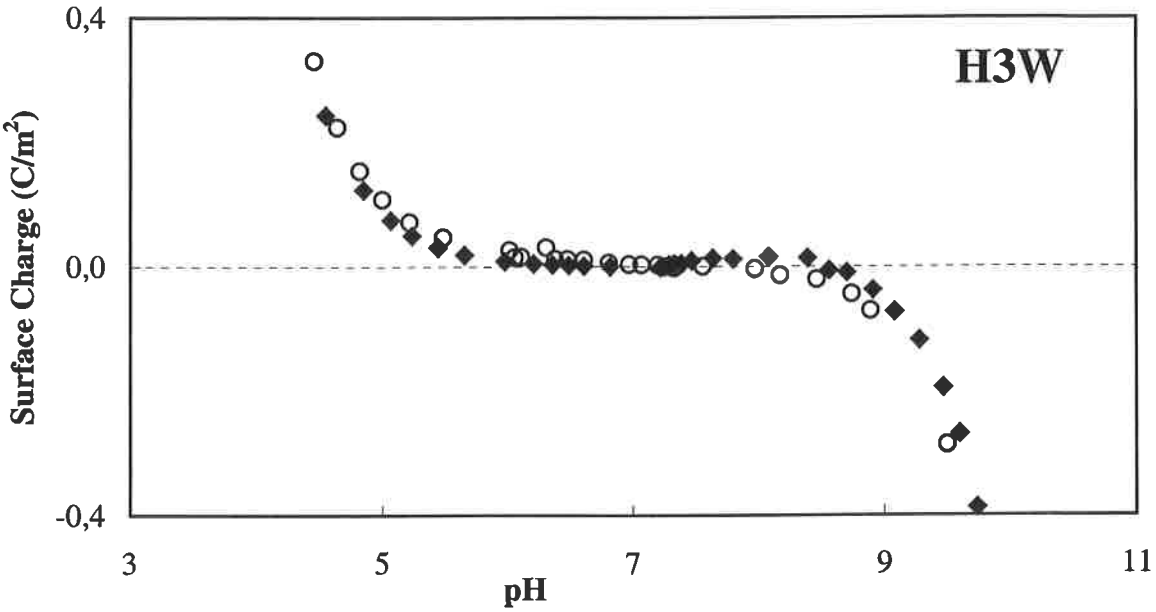
H3W
Surface Charge (C/m2)
0,4
0,0
-0,4
3
5
7
9
11
pH

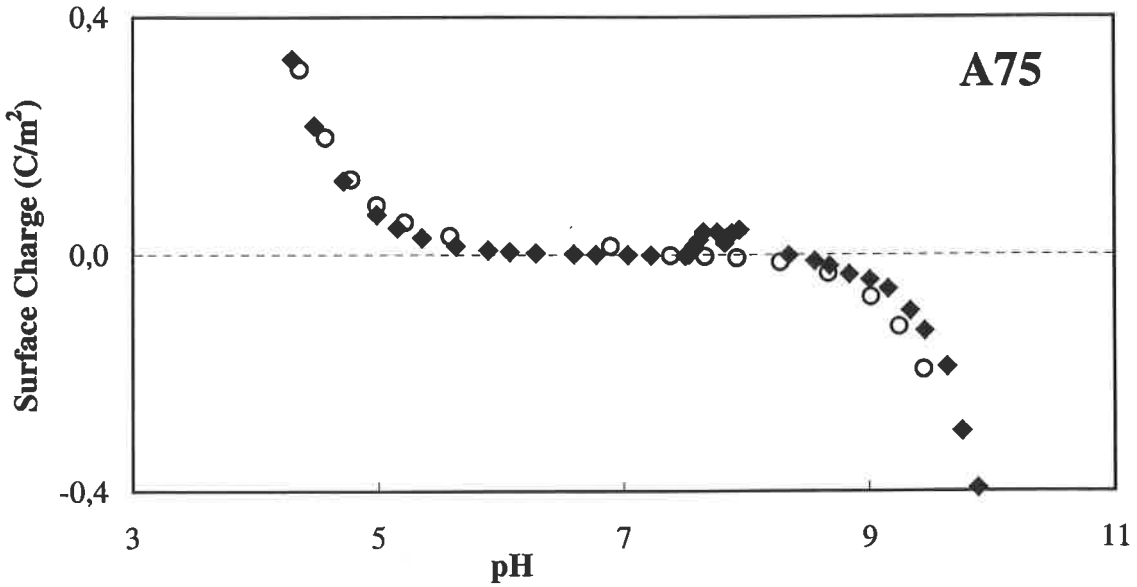
A75
Surface Charge (C/m2)
0,4
0,0
-0,4
3
5
7
9
11
pH

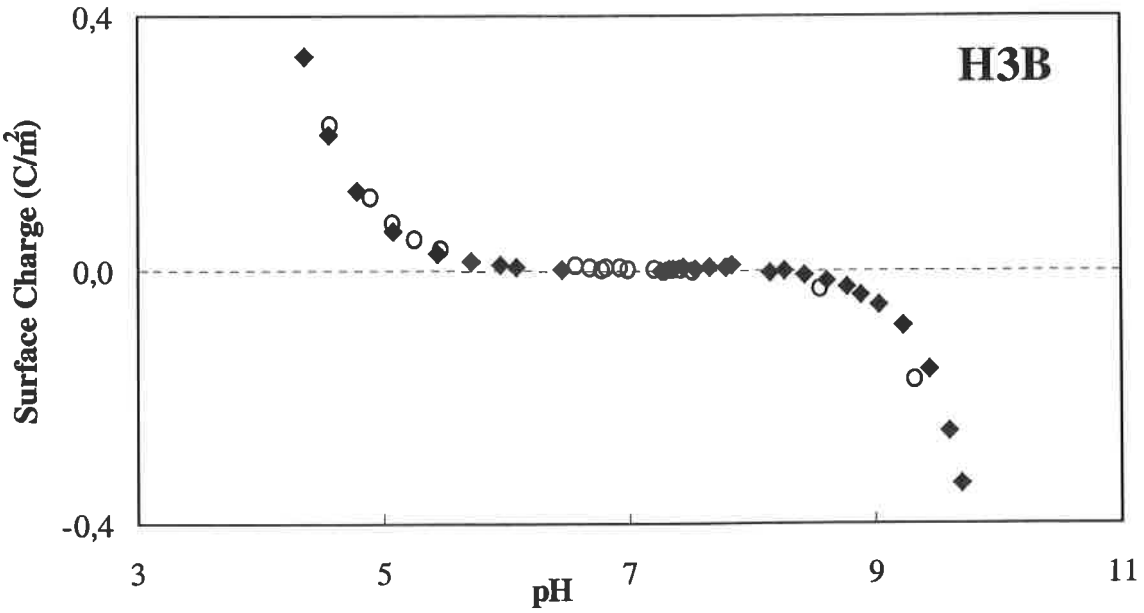
H3B
Surface Charge (C/m2)
0,4
0,0
-0,4
3
5
7
9
11
pH

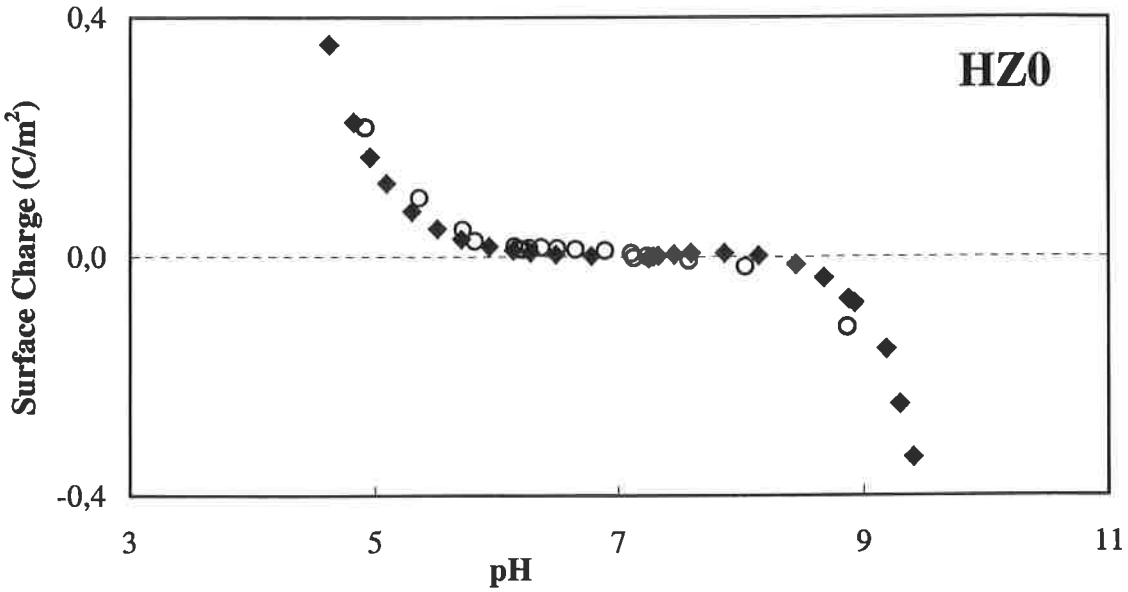
HZ0
Surface Charge (C/m²)
0,4
0,0
-0,4
3
5
7
9
11
pH

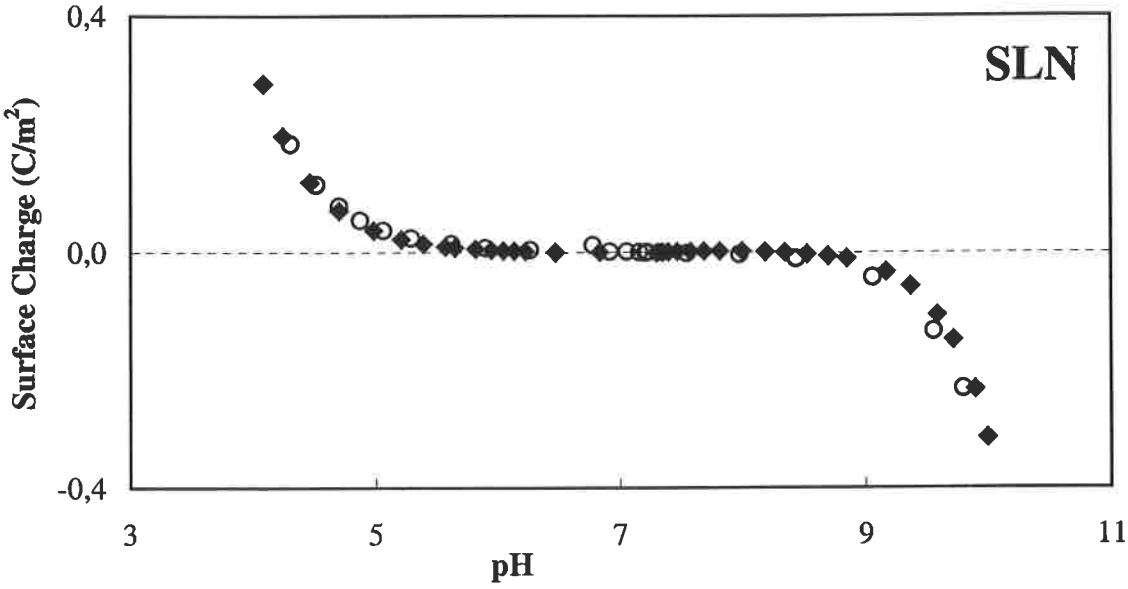
SLN
Surface Charge (C/m²)
0,4
0,0
-0,4
3
5
7
9
11
pH

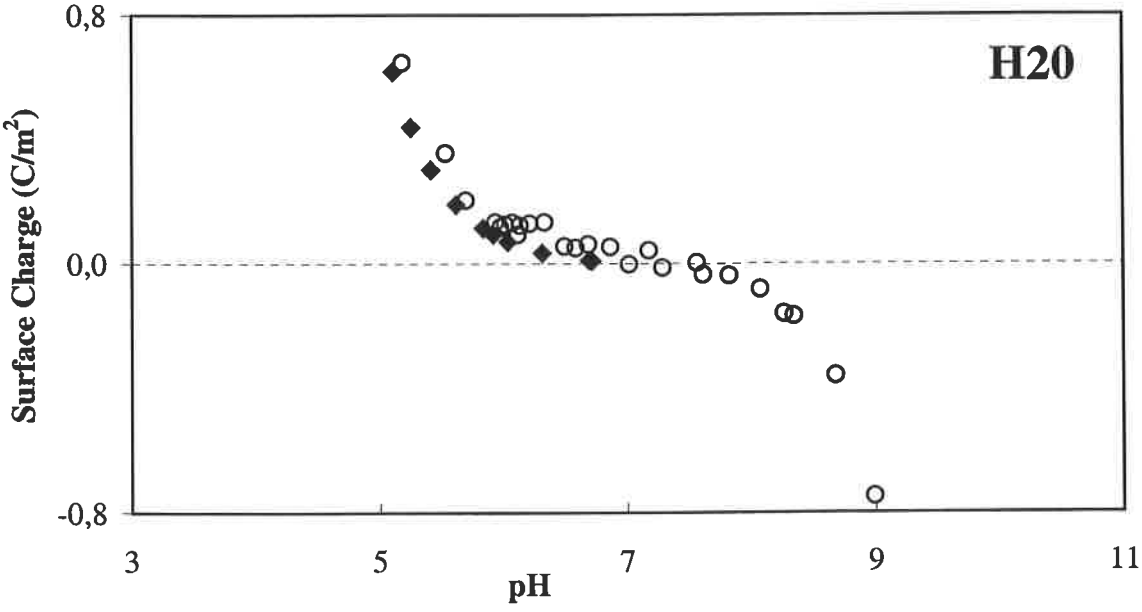
H20
Surface Charge (C/m²)
0,8
0,0
-0,8
3
5
7
9
11
pH

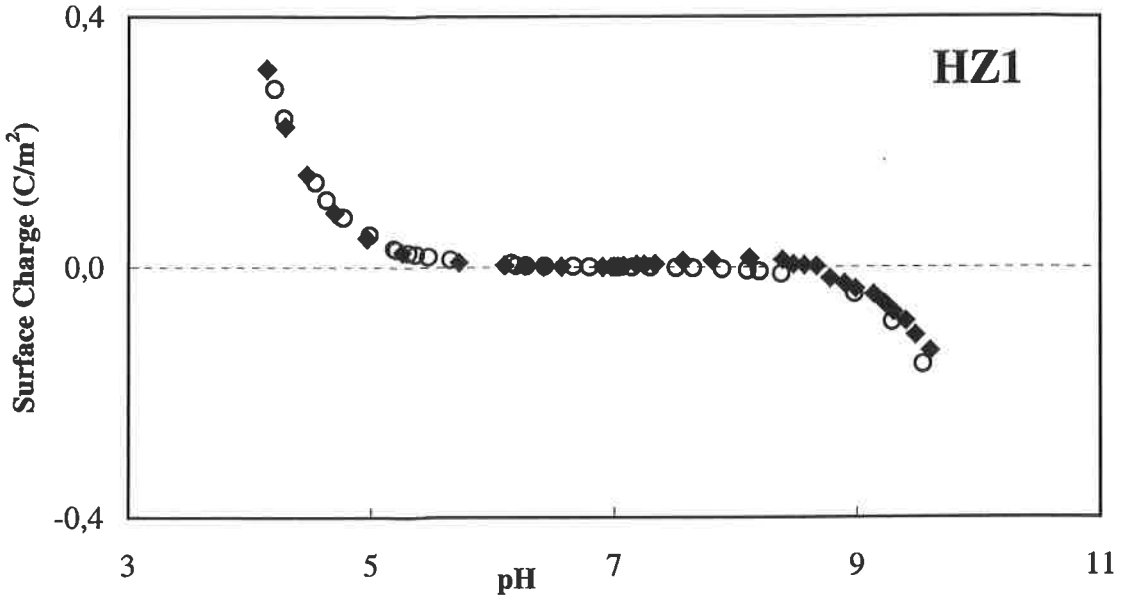
HZ1
0,4
0,0
-0,4
Surface Charge (C/m²)
3
5
7
9
11
pH

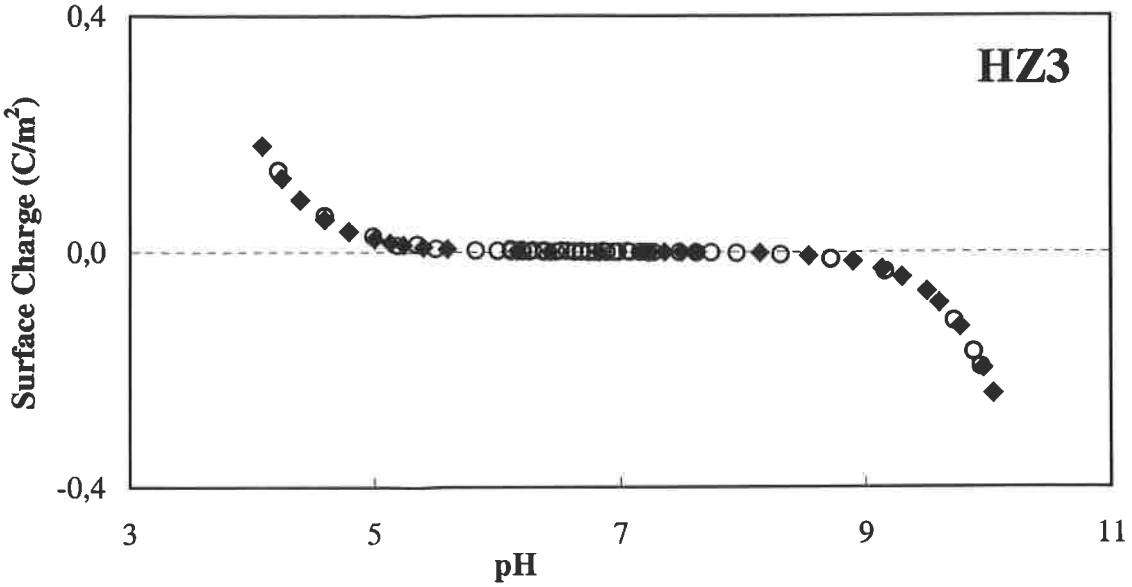
HZ3
0,4
0,0
-0,4
Surface Charge (C/m²)
3
5
7
9
11
pH

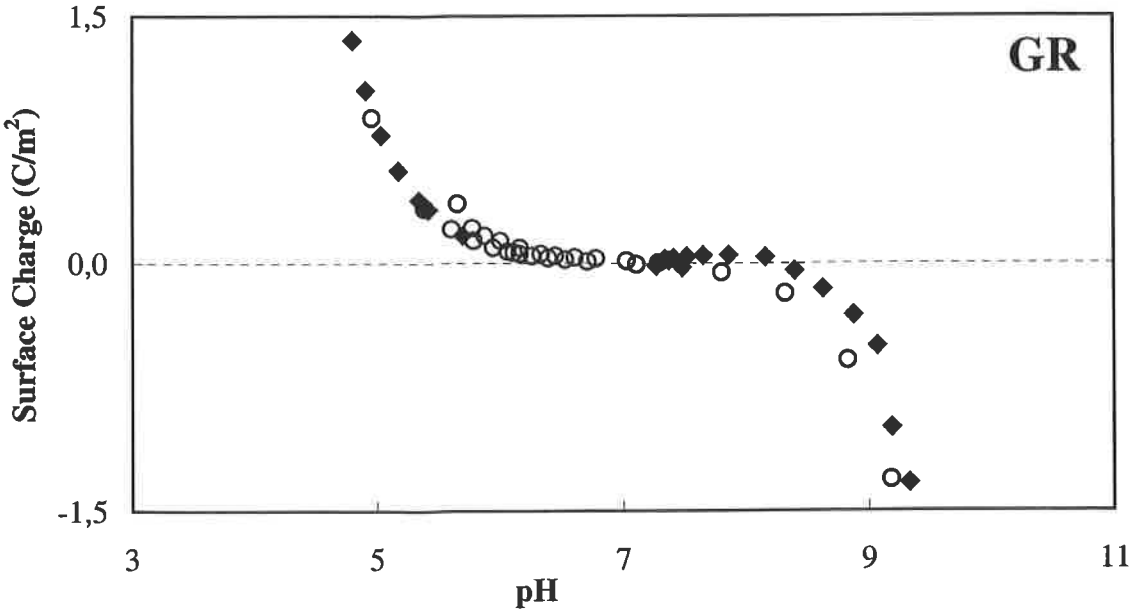
GR
1,5
0,0
-1,5
Surface Charge (C/m²)
3
5
7
9
11
pH

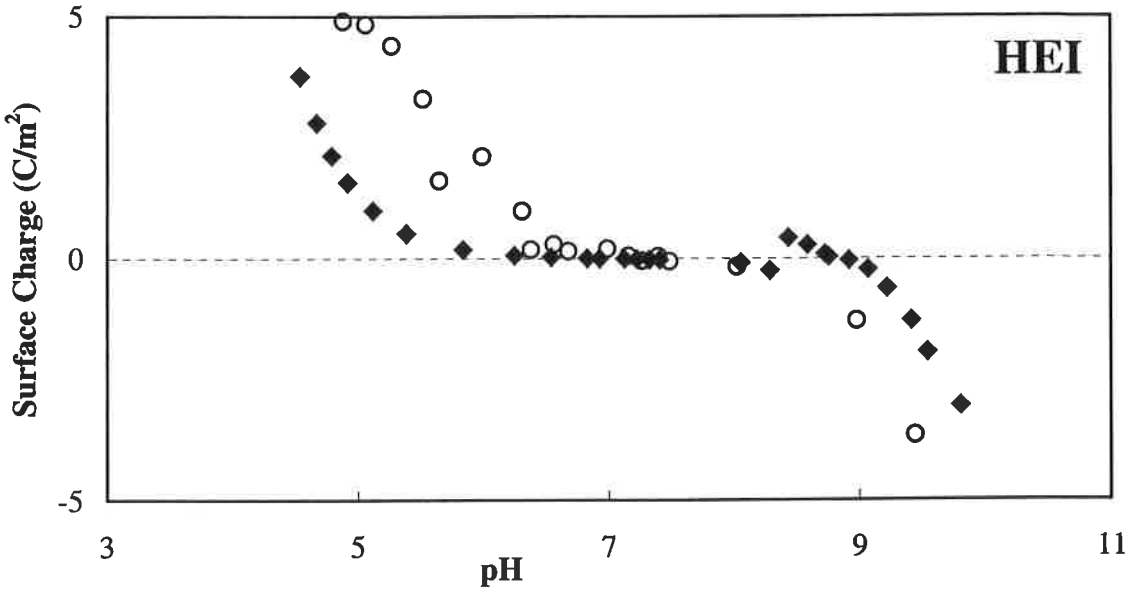
HEI
Surface Charge (C/m²)
5
0
-5
3
5
7
9
11
pH

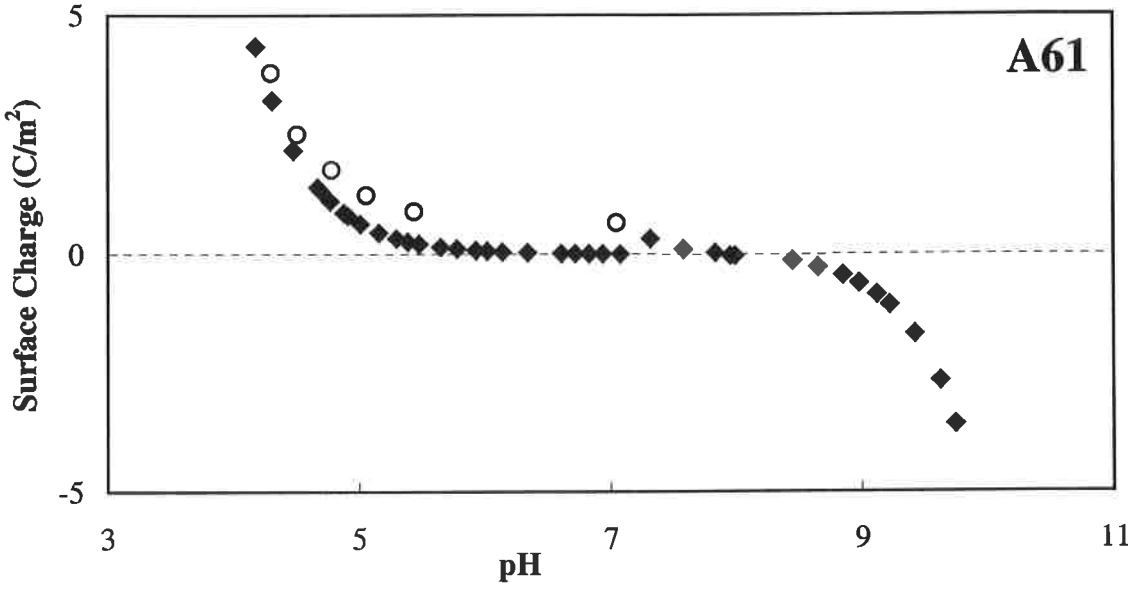
A61
Surface Charge (C/m²)
5
0
-5
3
5
7
9
11
pH

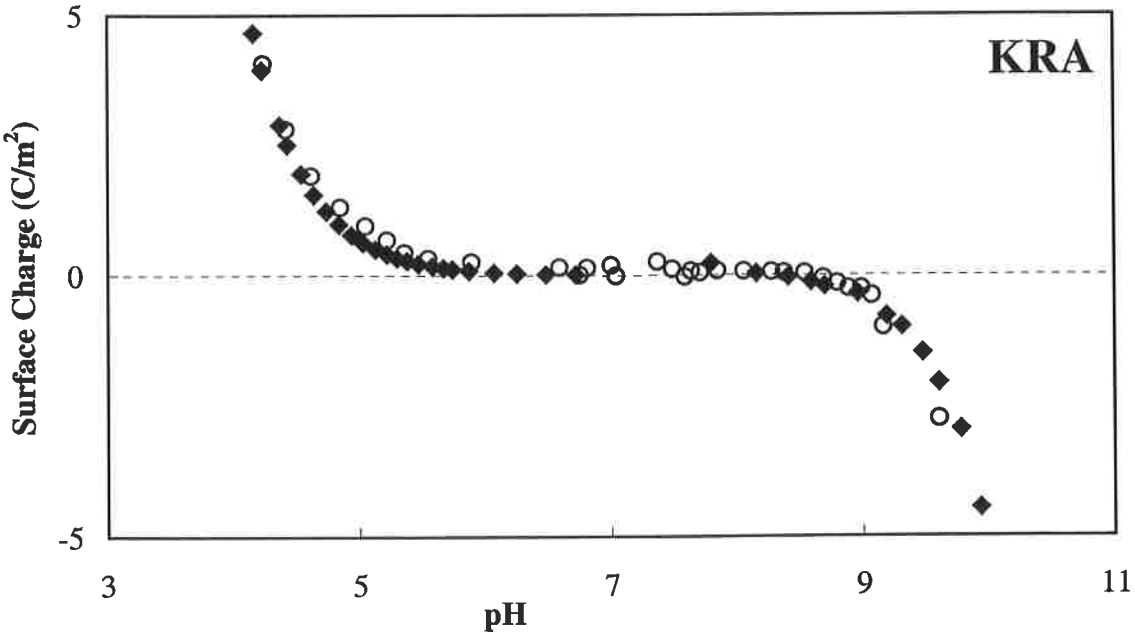
KRA
Surface Charge (C/m²)
5
0
-5
3
5
7
9
11
pH

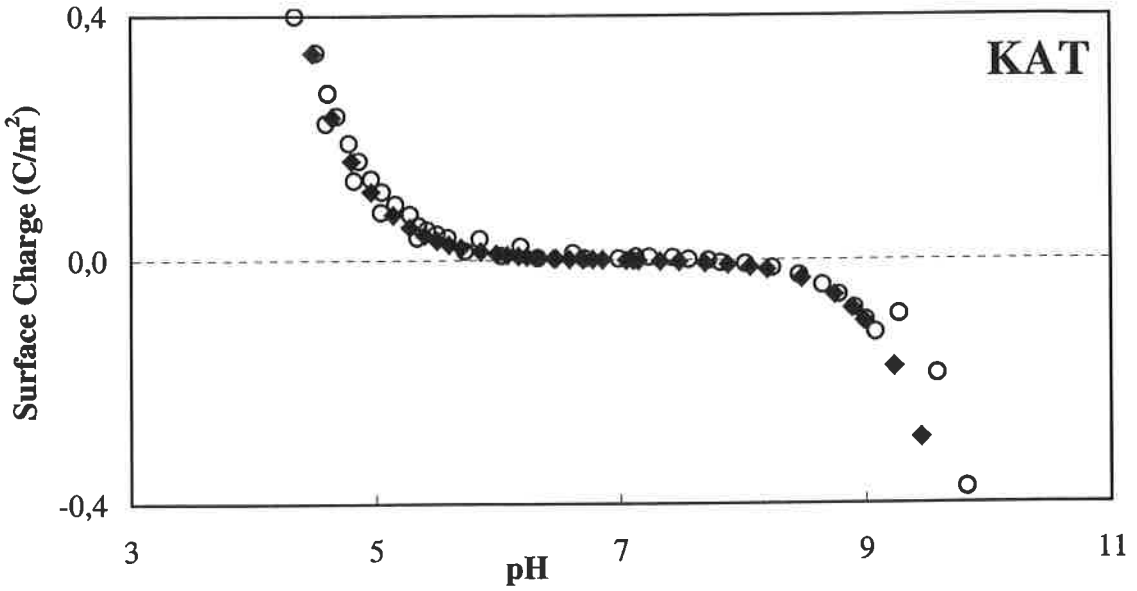
KAT
Surface Charge (C/m²)
0,4
0,0
-0,4
3
5
7
9
11
pH

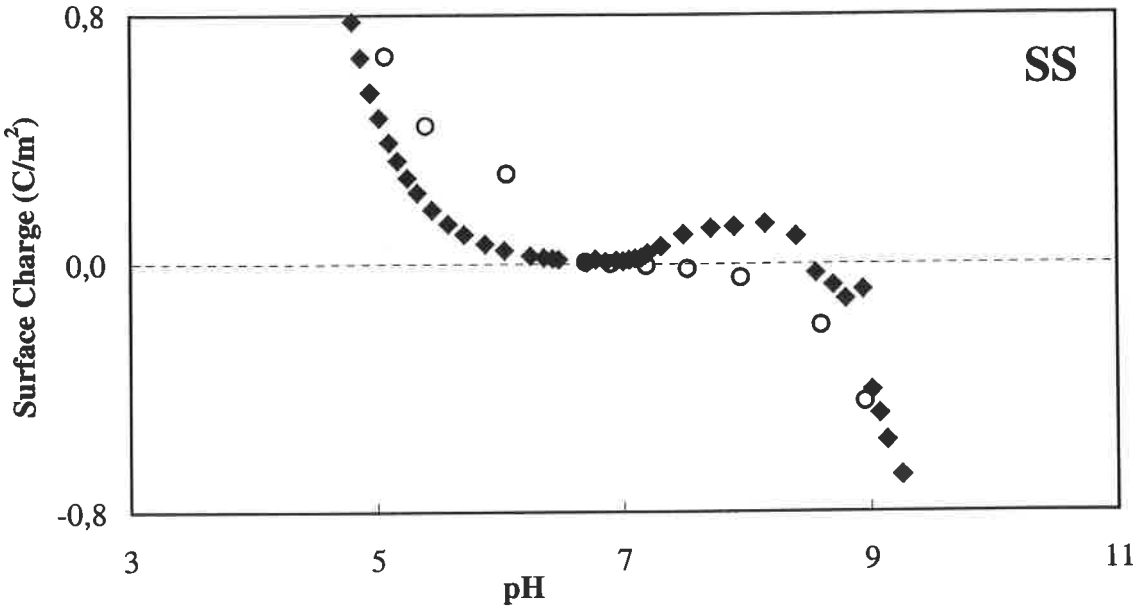
SS
Surface Charge (C/m²)
0,8
0,0
-0,8
3
5
7
9
11
pH

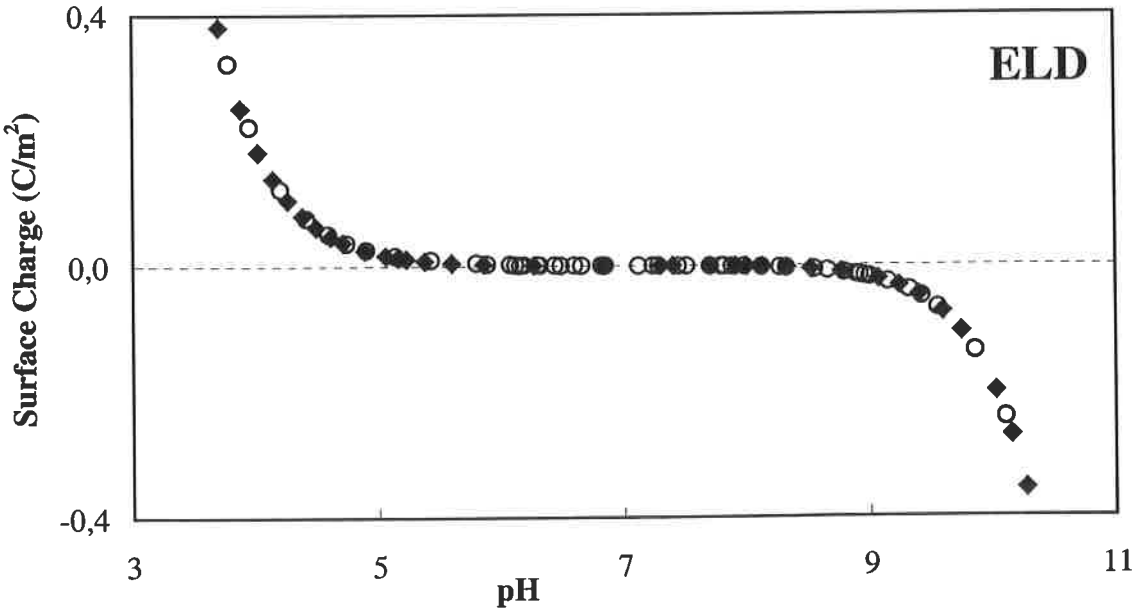
ELD
Surface Charge (C/m²)
0,4
0,0
-0,4
3
5
7
9
11
pH

Equilibrium Constants

Equilibrium constants for the dissolution of volcanic glasses are estimated assuming that non-framework cations are leached out of the glass leaving a hydrated surface gel enriched in network forming cations. It is this gel that undergoes eventual hydrolysis. Therefore the K_{HVG} values compiled in tables 6 and 7 refer to the hydrolysis reaction of this leached gel and not of the whole original glass, which does not attain thermodynamical equilibrium with the solution. The gel chemical formula consists of the glass network formers (Si and Al) and OH groups.

Table 6 The composition of the hydrated volcanic glasses (HVG), their hydrolysis reactions under acid conditions and the logarithm of the equilibrium constants (K_{HVG}) of these reactions used to estimate saturation indices (at 25°C)

Sample	volcanic name	Hydrolysis reaction for the HVG under **acid** conditions	log K_{HVG}
BT	rhyolite	$SiAl_{0.20}O_2(OH)_{0.61} + 0.61H^+ + 1.39H_2O = H_4SiO_4 + 0.20Al^{3+}$	-0.55
Ö62	rhyolite	$SiAl_{0.22}O_2(OH)_{0.65} + 0.65H^+ + 1.35H_2O = H_4SiO_4 + 0.22Al^{3+}$	-0.33
H1	rhyolite	$SiAl_{0.23}O_2(OH)_{0.69} + 0.69H^+ + 1.31H_2O = H_4SiO_4 + 0.23Al^{3+}$	-0.23
H3W	rhyolite	$SiAl_{0.23}O_2(OH)_{0.70} + 0.70H^+ + 1.30H_2O = H_4SiO_4 + 0.23Al^{3+}$	-0.23
A75	rhyolite	$SiAl_{0.21}O_2(OH)_{0.63} + 0.63H^+ + 1.37H_2O = H_4SiO_4 + 0.21Al^{3+}$	-0.44
H3B	dacite	$SiAl_{0.26}O_2(OH)_{0.78} + 0.78H^+ + 1.22H_2O = H_4SiO_4 + 0.26Al^{3+}$	0.10
HZ0	dacite	$SiAl_{0.29}O_2(OH)_{0.86} + 0.86H^+ + 1.14H_2O = H_4SiO_4 + 0.29Al^{3+}$	0.42
SLN	dacite	$SiAl_{0.27}O_2(OH)_{0.81} + 0.81H^+ + 1.19H_2O = H_4SiO_4 + 0.27Al^{3+}$	0.21
H20	basaltic andesite	$SiAl_{0.31}O_2(OH)_{0.93} + 0.93H^+ + 1.07H_2O = H_4SiO_4 + 0.31Al^{3+}$	0.64
HZ1	basaltic andesite	$SiAl_{0.32}O_2(OH)_{0.97} + 0.97H^+ + 1.03H_2O = H_4SiO_4 + 0.32Al^{3+}$	0.75
HZ3	basalt	$SiAl_{0.33}O_2(OH)_{0.99} + 0.99H^+ + 1.01H_2O = H_4SiO_4 + 0.33Al^{3+}$	0.85
GR	basalt	$SiAl_{0.32}O_2(OH)_{0.95} + 0.95H^+ + 1.05H_2O = H_4SiO_4 + 0.32Al^{3+}$	0.75
HEI	mugearite	$SiAl_{0.38}O_2(OH)_{1.13} + 1.13H^+ + 0.87H_2O = H_4SiO_4 + 0.38Al^{3+}$	1.39
A61	basalt	$SiAl_{0.30}O_2(OH)_{0.90} + 0.90H^+ + 1.10H_2O = H_4SiO_4 + 0.30Al^{3+}$	0.53
KRA	basalt	$SiAl_{0.32}O_2(OH)_{0.96} + 0.96H^+ + 1.04H_2O = H_4SiO_4 + 0.32Al^{3+}$	0.75
KAT	basalt	$SiAl_{0.32}O_2(OH)_{0.95} + 0.95H^+ + 1.05H_2O = H_4SiO_4 + 0.32Al^{3+}$	0.75
SS	basalt	$SiAl_{0.42}O_2(OH)_{1.25} + 1.25H^+ + 0.75H_2O = H_4SiO_4 + 0.42Al^{3+}$	1.83
ELD	basalt	$SiAl_{0.33}O_2(OH)_{1.00} + 1.00H^+ + 1.00H_2O = H_4SiO_4 + 0.33Al^{3+}$	0.85

Example of the calculation of ELD's K_{HVG}:
(amorphous) $SiO_2 + 2\ H_2O = H_4SiO_4$; log K –2.71 (PHREEQC)
(amorphous) $Al(OH)_3 + 3\ H^+ = Al^{3+} + 3\ H_2O$; log K 10.80 (PHREEQC)
=> 1(Si)·-2.71 + 0.33(Al)·10.80 = 0.85

Table 7 The composition of the hydrated volcanic glasses (HVG), their hydrolysis reactions under alkaline conditions and the logarithm of the equilibrium constants (K_{HVG}) of these reactions used to estimate saturation indices (at 25°C)

Sample	volcanic name	Hydrolysis reaction for the HVG under **alkaline** conditions	log K_{HVG}
BT	rhyolite	$SiAl_{0.20}O_2(OH)_{0.61} + 2H_2O + 0.20OH^- = H_4SiO_4^* + 0.20Al(OH)_4^-$	-2.29
Ö62	rhyolite	$SiAl_{0.22}O_2(OH)_{0.65} + 2H_2O + 0.22OH^- = H_4SiO_4^* + 0.22Al(OH)_4^-$	-2.25
H1	rhyolite	$SiAl_{0.23}O_2(OH)_{0.69} + 2H_2O + 0.23OH^- = H_4SiO_4^* + 0.23Al(OH)_4^-$	-2.23
H3W	rhyolite	$SiAl_{0.23}O_2(OH)_{0.70} + 2H_2O + 0.23OH^- = H_4SiO_4^* + 0.23Al(OH)_4^-$	-2.23
A75	rhyolite	$SiAl_{0.21}O_2(OH)_{0.63} + 2H_2O + 0.21OH^- = H_4SiO_4^* + 0.21Al(OH)_4^-$	-2.27
H3B	dacite	$SiAl_{0.26}O_2(OH)_{0.78} + 2H_2O + 0.26OH^- = H_4SiO_4^* + 0.26Al(OH)_4^-$	-2.16
HZ0	dacite	$SiAl_{0.29}O_2(OH)_{0.86} + 2H_2O + 0.29OH^- = H_4SiO_4^* + 0.29Al(OH)_4^-$	-2.10
SLN	dacite	$SiAl_{0.27}O_2(OH)_{0.81} + 2H_2O + 0.27OH^- = H_4SiO_4^* + 0.27Al(OH)_4^-$	-2.14
H20	basaltic andesite	$SiAl_{0.31}O_2(OH)_{0.93} + 2H_2O + 0.31OH^- = H_4SiO_4^* + 0.31Al(OH)_4^-$	-2.06
HZ1	basaltic andesite	$SiAl_{0.32}O_2(OH)_{0.97} + 2H_2O + 0.32OH^- = H_4SiO_4^* + 0.32Al(OH)_4^-$	-2.04
HZ3	basalt	$SiAl_{0.33}O_2(OH)_{0.99} + 2H_2O + 0.33OH^- = H_4SiO_4^* + 0.33Al(OH)_4^-$	-2.02
GR	basalt	$SiAl_{0.32}O_2(OH)_{0.95} + 2H_2O + 0.32OH^- = H_4SiO_4^* + 0.32Al(OH)_4^-$	-2.04
HEI	mugearite	$SiAl_{0.38}O_2(OH)_{1.13} + 2H_2O + 0.38OH^- = H_4SiO_4^* + 0.38Al(OH)_4^-$	-1.91
A61	basalt	$SiAl_{0.30}O_2(OH)_{0.90} + 2H_2O + 0.30OH^- = H_4SiO_4^* + 0.30Al(OH)_4^-$	-2.08
KRA	basalt	$SiAl_{0.32}O_2(OH)_{0.96} + 2H_2O + 0.32OH^- = H_4SiO_4^* + 0.32Al(OH)_4^-$	-2.04
KAT	basalt	$SiAl_{0.32}O_2(OH)_{0.95} + 2H_2O + 0.32OH^- = H_4SiO_4^* + 0.32Al(OH)_4^-$	-2.04
SS	basalt	$SiAl_{0.42}O_2(OH)_{1.25} + 2H_2O + 0.42OH^- = H_4SiO_4^* + 0.42Al(OH)_4^-$	-1.83
ELD	basalt	$SiAl_{0.33}O_2(OH)_{1.00} + 2H_2O + 0.33OH^- = H_4SiO_4^* + 0.33Al(OH)_4^-$	-2.02

Example of the calculation of ELD's K_{HVG}:
(amorphous) $SiO_2 + 2\ H_2O = H_4SiO_4$; log K –2.71 (PHREEQC)
(amorphous) $Al(OH)_3 + 3\ H^+ = Al^{3+} + 3\ H_2O$; log K 10.80 (PHREEQC)
$Al^{3+} + 4H_2O = Al(OH)_4^- + 4H^+$; log K –22.7 (PHREEQC)
$H^+ + OH^- = H_2O$; log K 14.0 (PHREEQC)
=> $1(Si)\cdot-2.71 + 0.33(Al)\cdot10.80 + 0.33(Al(OH)_4)\cdot-22.7 + 0.33(OH)\cdot14 = -2.02$

*Note that at basic pH: $H_4SiO_4 = H_3SiO_4^- + H^+$; log K –9.83 (PHREEQC)

Corrosion Resistance

There exist parameters that contribute to the corrosion stability of glass and which can be inferred from the glass chemical composition. For example, in pure silica each of the four oxygens that make up the silica tetrahedron is linked to another tetrahedron so that the molar silicon to oxygen ratio in the structure of the glass (**Si:O ratio**) is 0.5. There are no non-bridging oxygens (**NBO**) present and the structure is totally three-dimensionally polymerised, chemically very stable and corrosion resistant. As network modifiers are introduced into the glass, the Si:O ratio decreases and the number of NBO increases; with this the stability of the glass diminishes. In table 8 these two important and interrelated parameters are compiled for the 18 volcanic glasses.

Table 8 Compilation of the molar silicon to oxygen ratio and the non-bridging oxygens of the volcanic glasses

Sample	Si:O	NBO_{WM}	NBO_{JP}
BT	0.41	-0.01	-0.04
Ö62	0.40	0.03	0.16
H1	0.40	0.06	0.26
H3W	0.40	0.06	0.26
A75	0.39	0.10	0.44
H3B	0.38	0.10	0.40
HZ0	0.36	0.18	0.57
SLN	0.37	0.17	0.59
H20	0.33	0.41	0.91
HZ1	0.33	0.33	0.76
HZ3	0.32	0.41	0.87
GR	0.31	0.74	1.23
HEI	0.31	0.47	0.92
A61	0.31	0.68	1.17
KRA	0.31	0.76	1.22
KAT	0.30	0.84	1.30
SS	0.29	0.73	1.12
ELD	0.29	0.81	1.23

The Si:O ratio is calculated:

$$Si:O = \frac{wt\%(SiO_2)}{M(SiO_2)\cdot\Sigma\frac{wt\%(i)\cdot n(i)}{M(i)}}$$

where (i) is any major oxide constituent apart from SiO_2, wt% stands for the weight fraction in percentage of the oxide, M is the molecular weight, and n the number of oxygens in the formula of the oxide.

For the number of NBO (based on *molar %*) two equations were employed:

$$NBO_{WM} = \frac{2(Na_2O + K_2O + CaO + MgO + MnO + FeO - Al_2O_3 - Fe_2O_3) + 4\cdot TiO_2}{(SiO_2 + 2\cdot Al_2O_3 + 2\cdot Fe_2O_3)}$$

This equation is a slightly altered version of the one proposed by White and Minser (1984). However, their equation ignored TiO_2 and this major oxide has been incorporated into this equation. Likewise, Jantzen and Plodinec (1984) modified the equation of White and Minser to calculate NBO of nuclear waste glasses. Stripped of any oxides whose concentrations are negligible (BaO, Cs_2O, Li_2O, SrO, UO_2, ZrO_2) their version was also utilized to calculate NBO:

$$NBO_{JP} = \frac{2(Na_2O + K_2O + CaO + MgO + MnO + FeO - Al_2O_3 - Fe_2O_3) + 4\cdot(TiO_2)}{\text{oxide mol sum}}$$

Note that the difference between both equations lies in the denominator.

References

Guy C. and Schott J. (1989) Multisite surface reaction versus transport control during hydrolysis of a complex oxide. *Chem. Geol.* **78**, 181-204.

Jantzen C. M. and Plodinec M. J. (1984) Thermodynamic model of natural, medieval and nuclear waste glass durability. *J. Non-Cryst. Solids* **67**, 207-223.

van den Bogaard P. and Schirnick C. (1995) $^{40}Ar/^{39}Ar$ laser probe ages of Bishop Tuff quartz phenocrysts substantiate long-lived silicic magma chamber at Long Valley, United States. *Geology* **23**, 759-762.

White W. B. and Minser D. G. (1984) Raman spectra and structure of natural glass. *J. Non-Cryst. Solids* **67**, 45-59.

Wilson C. J. N. and Hildreth W. (1997) The Bishop Tuff: New insights and implications from eruptive stratigraphy. *J. Geol.* **105**, 407-439.

Wolff-Boenisch D., Gislason S. R., Oelkers E. H., and Putnis C. V. (2004a) The dissolution rates of natural glasses as a function of their composition at pH 4 and 10.6, and temperatures from 25 to 74°C. *Geochim. Cosmochim. Acta*, in press.

Wolff-Boenisch D., Gislason S. R., and Oelkers E. H. (2004b) The effect of fluoride on the geometric surface area normalized dissolution rates of natural volcanic glasses at pH 4 and 25°C. *Geochim. Cosmochim. Acta*, in press.